

# Northumbria Research Link

Citation: Suntharalingam, Thadshajini, Upasiri, Irindu, Nagaratnam, Brabha, Poologanathan, Keerthan, Perampalam, Gatheeshgar, Tsavdaridis, Konstantinos and Perera, Dilini (2022) Finite Element Modelling to predict the Fire performance of Bio-inspired 3D Printed Concrete wall panels exposed to realistic fire. *Buildings*, 12 (2). p. 111. ISSN 2075-5309

Published by: MDPI

URL: <https://doi.org/10.3390/buildings12020111>  
<<https://doi.org/10.3390/buildings12020111>>

This version was downloaded from Northumbria Research Link:  
<http://nrl.northumbria.ac.uk/id/eprint/48214/>

Northumbria University has developed Northumbria Research Link (NRL) to enable users to access the University's research output. Copyright © and moral rights for items on NRL are retained by the individual author(s) and/or other copyright owners. Single copies of full items can be reproduced, displayed or performed, and given to third parties in any format or medium for personal research or study, educational, or not-for-profit purposes without prior permission or charge, provided the authors, title and full bibliographic details are given, as well as a hyperlink and/or URL to the original metadata page. The content must not be changed in any way. Full items must not be sold commercially in any format or medium without formal permission of the copyright holder. The full policy is available online: <http://nrl.northumbria.ac.uk/policies.html>

This document may differ from the final, published version of the research and has been made available online in accordance with publisher policies. To read and/or cite from the published version of the research, please visit the publisher's website (a subscription may be required.)

## **Finite Element Modelling to predict the Fire performance of Bio-inspired 3D Printed Concrete wall panels exposed to realistic fire**

Suntharalingam Thadshajini<sup>(a)</sup>, Irindu Upasiri<sup>(b)</sup>, Brabha Nagaratnam<sup>(a)\*</sup>, Keerthan Poologanathan<sup>(a)</sup>, Perampalam Gatheeshgar<sup>(a)</sup>, Konstantinos Tsavdaridis<sup>(c)</sup>, Dilini Nuwanthika<sup>(a)</sup>

(a) Northumbria University, Newcastle upon Tyne, NE18ST, United Kingdom

(b) University of Sri Jayewardenepura, Dehiwala-Mount Lavinia, Sri Lanka

(c) University of Leeds, United Kingdom

\* E-mail: [brabha.nagaratnam@northumbria.ac.uk](mailto:brabha.nagaratnam@northumbria.ac.uk)

**Abstract:** The large-scale additive manufacturing (AM), well-recognized as 3D concrete printing is developing and therefore gained intensive research attention. However, this technology is requiring appropriate specifications and standard guidelines. Furthermore, the performance of printable concrete in elevated temperature circumstances is still not explored extensively. Hence, the authors believe that there is a demand for a set of standardized findings through the support of experiments and numerical modelling of fire performance of 3D printed concrete structural elements. In general, fire experiments and simulations focus on ISO 834 standard fire. However, this may not simulate the real fire behaviour of 3D printed concrete walls. With the aim of bridge this knowledge disparity, this article presents an analysis on the fire performance of 3D printed concrete walls with biomimetic hollow cross sections exposed to individual realistic fire circumstances. The fire performance of the non-load bearing 3D printed concrete wall was identified via developing a suitable numerical heat transfer model. The legitimacy of the developed numerical model was proved by comparing the time-temperature changes with existing results derived from fire experiments on 3D printed concrete walls. A parametric study of 96 numerical models was, consequently, performed including different 3D printed concrete wall configurations under 4 fire curves (standard, prolong, rapid, hydrocarbon fire). 3D printed concrete walls and mineral wool cavity infilled wall panels showed enhanced fire performance. Moreover, Cellular structures demonstrated in superior insulation fire rating compared to other configurations.

**Keywords:** 3D Concrete Printing, Bio-inspired structures, Fire performance, Real Fire, Finite element modelling, Insulation fire rating.

## **1. Introduction**

### **1.1 3D Concrete Printing (3DCP)**

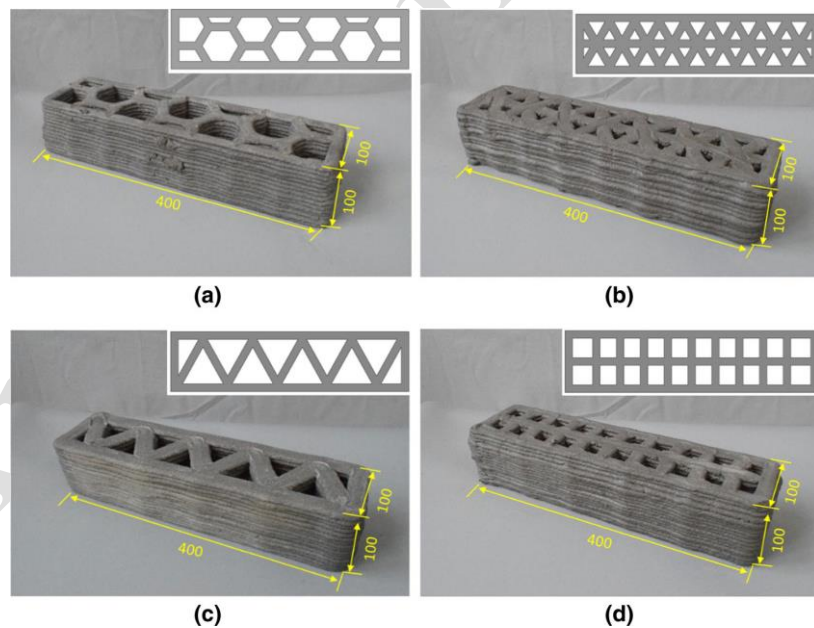
Additive Manufacturing (AM) technology in construction is generally known as Three-dimensional Concrete Printing (3DCP) has shown a rapid development over the last decade, following the digital technologies such as AI (Artificial Intelligence), BIM (Building Information Modelling) and VR (Virtual Reality) [1]. The word 3D Concrete Printing (3DCP) indicates various tools those build 3D objects by stacking concrete layers until the required geometry is achieved [2, 3].

Compared to conventional construction methods, 3DCP has shown technical, economic, social, and environmental benefits. This technique has offered room for creativity and design freedom for architects and engineers to developed intricate, customized structures that are previously neither possible nor achievable with standard formwork along with topological optimization [4-7]. In addition, the bespoke advantages of 3DCP are potential higher quality of construction, reduced construction time, innovative structures at lower associated costs, development of material-minimized, resource-saving structures, optimization of thermal and acoustic properties of the building, reduction of arduous manpower and hence increased the labour efficiency and safety. This process also reduces the adverse impacts on environmental by direct use of natural materials, reduced transportation, the reduction of waste, and minimal energy usage [1, 3, 5, 7-15].

When emerging a novel technology, the basic constraints including desired mechanical behaviour, dimensional stability, fire resistance and durability must be studied comprehensively. Moreover, the knowledge difference between largescale 3DCP and laboratory 3DCP is still limited with lack of design rules and guidelines. In addition, it is also crucial to envisage its impact on the environment, energy consumption, thermal efficiency, sustainability and resilience for long-term accomplishment [7]. Hence, it is imperative for the built environment to achieve the required structural and thermal performance while reducing substantial energy consumption [16, 17]. As a solution, construction industry has embraced the bio-inspired designs which can provide improved energy performance with lessened adverse effects on the environment [5, 18, 19]. The integration of biomimicry in construction be able to noticed in the use of cellular structures or lattice structures, which commonly offer improved stiffness and lightness properties with better thermal and acoustical characteristics [5].

## 1.2 Bio-inspired design for 3DCP

In nature, there are many biological structures which are complicated in shape but naturally optimized to provide different purposes with excellent mechanical properties [20]. However, such nature-inspired design entities are complicated and are challenging to replicate with normal formwork concrete fabrication. Current advances in 3DCP have provided a pathway to build arbitrary and multi-material geometries with some highly exceptional design strategies witnessed in nature and have endorsed a surge in the research of biomimetic design [21]. Lately, an growing number of studies on the construction and assessment of bio-inspired structures have been performed owing to the development of 3DCP [12, 22]. Plessis et al. [23] comprehensively reviewed the potential for the integration of bio-inspired design for 3D concrete printing. The study claims that extrusion-based 3DCP works perfectly to produce simple cellular structures. Wang et al. [24] 3D printed and tested some wall panels with bio-inspired hollow sections such as lattice, triangular, truss and cellular for mechanical behaviour (Fig 1). Panda et al. [25] experimentally analyzed the mechanical properties such as yield strength and modulus of elasticity of hexagonal honeycomb cellular structures 3D printed using Fused Deposition Method (FDM).



**Fig 1: 3D printed samples (a) Cellular; (b) Triangular; (c) Truss; (d) Lattice [24] (unit: mm)**

Moini et al. [26] 3D printed some bio-inspired designs like honeycomb, cellular panel, and bouligand shapes using cementitious material and found that these sections have improved the crack resistance, toughness and reduced the inelastic deflection and failure by over 50% compared to the conventional manufactured elements [26] (Fig 2).

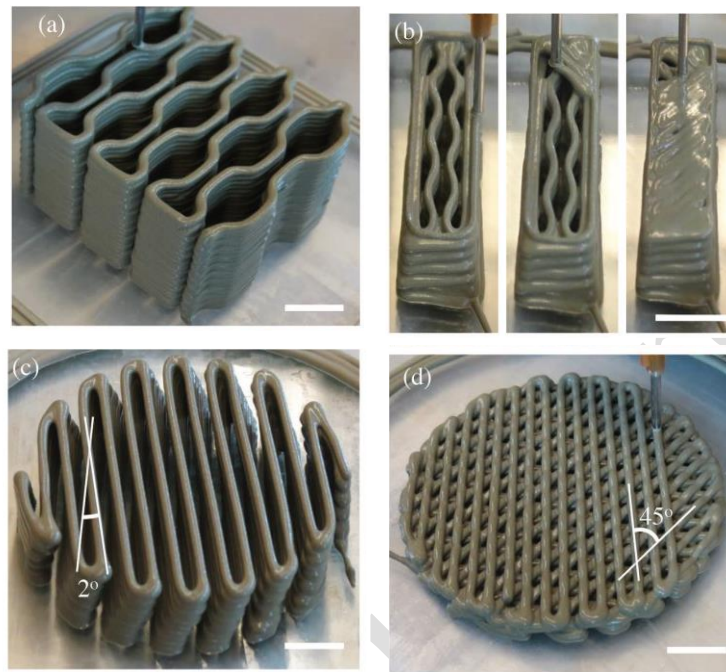


Fig 2: (a)Honeycomb; (b)Cellular panel; (c)Bouligand shape (2°); (d)Bouligand shape (45°); [26]

### 1.3 Fire Performance of construction materials

Many concepts and design methods have been established in order to identify the structural performance of 3D printed concrete wall panels at ambient temperature. However, the fire behaviour and thermal performance of these structures under elevated temperature have not been investigated sufficient to bridge the knowledge gap with real life practice.

The fire resistance and thermal performance of normal weight, light weight concrete and steel have been analysed significantly with well-established design guidelines for elevated temperature [27-34]. These studies are based on the comparative fire behaviour of light weight and normal concrete composite structures [31]; large scale experiments to examine the behaviour of concrete elements under standard fire condition [33]; effect of raised temperature on concrete bond strength [27]; numerical analysis of fire performance of Composite Sandwich Panels (CSP) under standard fire and hydrocarbon fire [28]; effect of hydrocarbon fire on the high strength geopolymer concrete wall panels [29] and thermal analysis of multi-layer walls [34].

In terms of steel material, Steau et al. [35] presented the thermal properties of carbon steels, which are generally applied for cold-formed LSF (Light gauge Steel) Frame systems. Also, Gunalan and Mahendran [36] predicted the fire resistance levels (FRL) cold-formed steel wall panels. LSF standard fire. Steau et al. [37] experimentally studied the fire resistant board structures exposed to standard fire to achieve higher fire resistance levels FRL. Gunalan et al. [38] experimentally studied the fire performance of load bearing cold-formed steel wall panels under standard fire and Ariyanayagam and Mahendran [39] studied that under realistic design fires and established fire design rules [40]. Ariyanayagam and Mahendran [41] also investigated the impact of cavity insulation on the fire resistance of LSF walls and found that the use of cavity insulation enhanced the FRL of non-load bearing walls, though it considerably reduced that of load bearing walls. In addition, experimental analyses of non-load bearing LSF walls in standard fire [42-44] and development of a large variety of fire performance data of LSF walls using finite element analysis (FEA) [45-49] are available for steel structures.

Though the standard fire curve has been used for centuries to determine the FRL of building elements, actual FRL of building components subjected to real fires is considerably less than that obtained from standard fire tests [40, 47]. Hence, ISO 834 standard fire test regulation are incompatible to evaluate the fire performance of 3D printed concrete walls in terms of the highest temperature and the correspondence time taken to reach that highest temperature [50].

#### **1.4 Performance of 3DCP Structures under elevated temperature**

The elevated-temperature thermo-mechanical behaviour of 3D printed concrete is anticipated to be distinct from that of normal concrete at elevated temperatures due to its special mix design, fabrication process and the uneven distribution of pore structure [30, 51, 52]. However, very few research are found for assessing the fire performance of 3DCP. Hence, it is vital to understand the effects of this new layer-based construction technique on the fire performance of 3D printed concrete elements.

Cicione et al. [53] pioneered the experimental evaluation of fire behaviour of 3DCP. The authors heated six samples of 3D printed concrete and three samples of mould casted using radiant panels and identified that the 3D printed concrete samples are experienced thermal-mechanical spalling in the form of the interlayer delamination. Furthermore, Cicione et al. [54] investigated the impact of transverse confinement and longitudinal confinement (boundary conditions) on the inter layer bond of 3D printed concrete elements at elevated temperatures through experiments. Weng et al. [52] conducted an experimental research to investigate the

printability and fire performance of 3D printed fibre reinforced cementitious composites under elevated temperatures. In addition, Pessoa et al. [5] conducted a systematic review of the thermal performance and thermal efficiency of 3D printed concrete buildings. Yazyev et al. [11] proposed a thermal engineering calculation to determine the thermal properties and surface quality of 3D printed concrete wall panels with a total width of 150 mm with an internal air layer with 75 mm thickness. Also, Xiao et al. [51] experimentally investigated the mechanical and microstructural development of 3D printed concrete under extremely high-temperature environments. The main findings from the study are 3D printed concrete experienced layer delamination at elevated temperature instead of spalling failure and temperature impacts on the microstructure of 3D printed concrete are notable temperature over 400 °C.

Sun et al. [55] performed an on-site full-scale thermographic inspection and heat transfer monitoring experiment to investigate the thermal performance of a real 3D printed concrete prototype building. The results revealed extremely non-uniform temperature dispersal on the outer wall surface of the examined house and inadequate thermal insulating performance. Moreover, Kaszynka et al. [56] determined the thermal properties of 3D printed concrete wall with High Performance Concrete (HPC) and insulated with mineral wool as it achieves the thermal-humidity conditions of traditional type of walls such as insulated brick, concrete and stud walls. The study found that the lower thickness (8cm) 3D printed concrete wall met the same thermal requirements compared to traditional masonry or concrete walls (14 cm) with mineral wool insulation. Hence, further research is quite required to investigate the thermal properties of 3D printed concrete elements, and the necessity of additional insulation system.

Furet et al. [1] proposed a new advanced technology Batiprint3DTM of producing a 3D printed intricate wall panel arrangement of a printed concrete wall encased with two polyurethane foam printed outer walls to offer both an internal insulation and external insulation to the structure without necessitating thermal bridges. Thus, the construction cost could be reduced by around 20% compared to that of the masonry blocks with insulation [1]. Kaszynka et al. [56] constructed a wall panel with 5 cm mineral wool and 14 cm polyurethane foam sandwiched between the 3D printed concrete layers with 3 cm. Yang et al. [57] proposed a novel hybrid heat-storage system to overcome insulation restrictions aroused in nonlinear 3D printed concrete structures.

In addition, Alchaar and Al-Tamimi [58] studied the compressive, flexural, and interlayer bond strengths variation of 3D printed concrete with increasing ambient temperature. Results revealed that hot weather accelerated the water evaporation which led to surface dryness, which

instigated the reduction of interlayer bond and compressive strength whereas, the flexural strength was increased by 18% at elevated temperatures associated to the ambient temperature samples due to the lesser material viscosities and better fibre orientation.

It is also vital to study the enduring sustainability of structures manufactured with 3DCP technique. Therefore, it is important to study associated with environmental sustainability specifically thermal comfort, acoustic performance, and structural energy efficiency, which influence the indoor environment quality. Marais et al. [59] have performed a computational evaluation of 3D printed concrete wall structures with cavity for thermal performance and presented thermal improvement strategies. Also, the results showed that the solid light weight foam concrete wall showed better thermal performance compared to 3D printed light weight foam concrete walls with large wide cavities. However, the reduction of cavity widths leads to enhanced thermal insulation. Mahadevan [60] conducted a study to examine the energy efficiency and thermal comfort of a building constructed using 3D printable concrete, M25 strength concrete, and brick masonry and claimed that the thermal performance of the 3D printed concrete structure is not persuasively appropriate in the long term compared to other materials. This encourages the need for further in-depth research in 3D printed concrete structures with environmental sustainability.

However, the performance of innovative biomimetic 3DCP structures about fire resistance and thermal performance is very limited to date. Also, the majority of research on 3D printed concrete has been experimental as far as this, with not much attention given to computational simulations. Furthermore, the fire performance of 3D printed concrete walls varies with numerous factors such as printable material composition, material density, wall thickness, wall cross sectional arrangements and the type of insulation. Therefore, authors have previously investigated some 3D printed concrete non-load bearing wall panels with different cross-sectional configurations such as triangular, lattice and sinusoid concentrating on investigating the fire resistance and thermal behaviour under standard fire condition and different real fire circumstances. (i.e., hydrocarbon fire, rapid fire, and prolonged fire) [16, 17, 30, 50].

### **1.5 Scope of the Study**

This paper aims to broaden the recent numerical analysis of the fire performance of 3D printed concrete non-load bearing wall panels. Thus, bio-inspired hollow cross sections under realistic fire curves were incorporated in this study. Abide by currently available geometries of 3D printed concrete walls in the construction industry and the cavity provisions proposed by Wang



et al.[24], this study numerically examines the fire behaviour of the advanced wall configurations. The developed heat transfer numerical model using Abaqus finite element software [61], is verified with the experimental outcomes from Cicione et al. [30, 53]. The precision of the developed computational framework is validated through comparing the time-temperature variation with existing fire test results. Additionally, parametric modelling is performed to have a thorough understanding on the effect of different cross sections with 96 numerical models under 4 real fire situations including standard, hydrocarbon fire, rapid and prolong with concrete density  $2400 \text{ kg/m}^3$ . Following the introduction, a methodology for developing FE model and the validation of the developed model with the existing experimental results are described in Section 2. Then, the numerical outcomes of the fire performance of 3D printed wall panels are discussed and compared. Finally, the main findings of this research are stated in the last section.

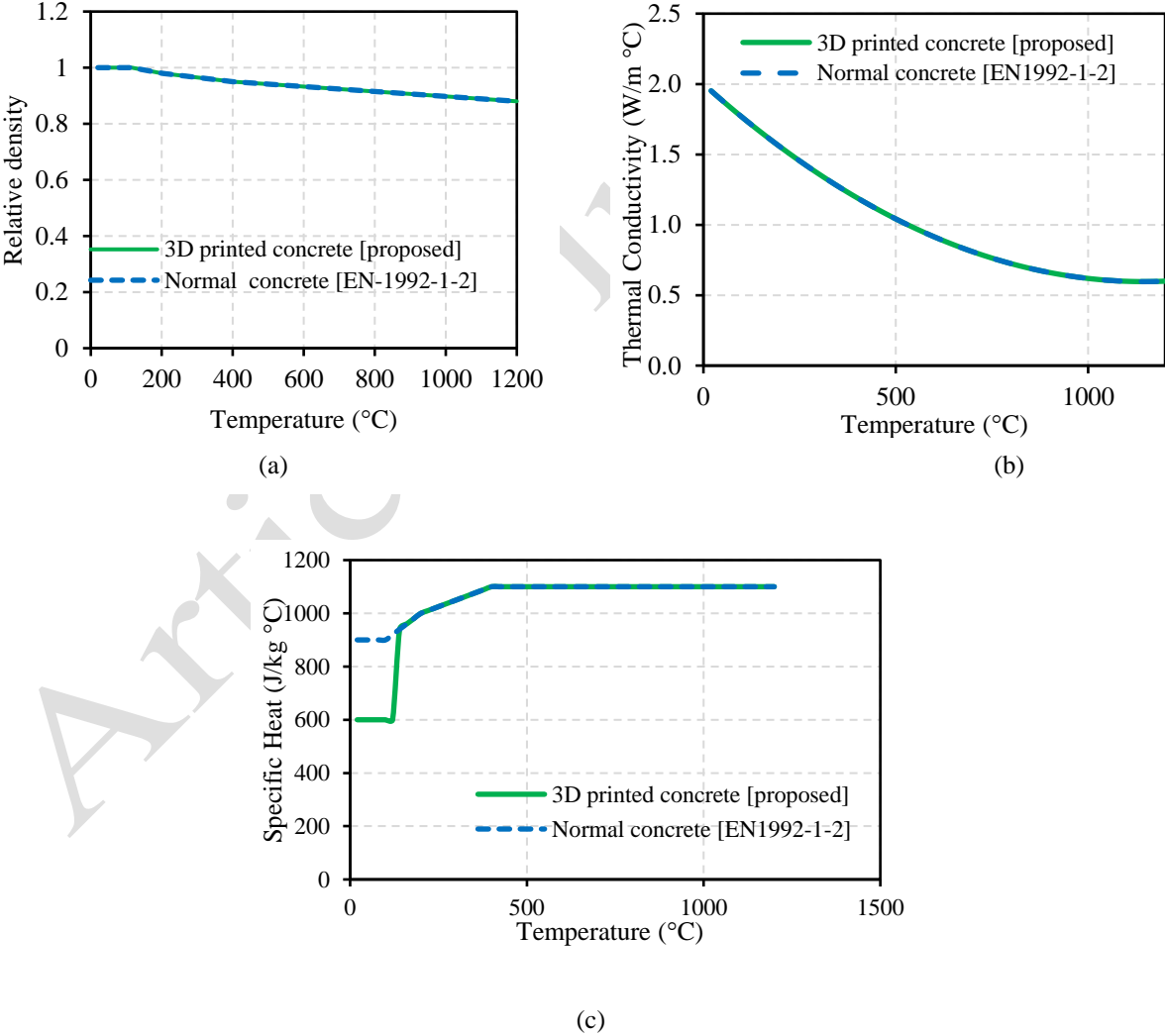
## **2. Finite Element Model development**

This section describes the development of FE heat transfer model of 3D concrete printed walls. Six different wall configurations: cavity and cavity filled with mineral wool insulation material were studied via FE analysis. Marais et al. [59] identified that if the temperature is consistent along the exterior surface of the 3D printed wall panel, the three-dimensional (3D) problem can be simplified to a two-dimensional (2D) problem, with assigning suitable thermal properties and boundary conditions. Hence, 2D heat transfer analysis was conducted to evaluate the insulation fire performance of the 3D printed walls in the FEM package ABAQUS [61]. Four types of fire conditions, standard fire, hydrocarbon fire, rapid-fire and prolonged fire, were applied to the 3D printed wall configurations. The temperature variation of the unexposed surface was evaluated. Based on the unexposed surface temperature increment, insulation fire rating was determined.

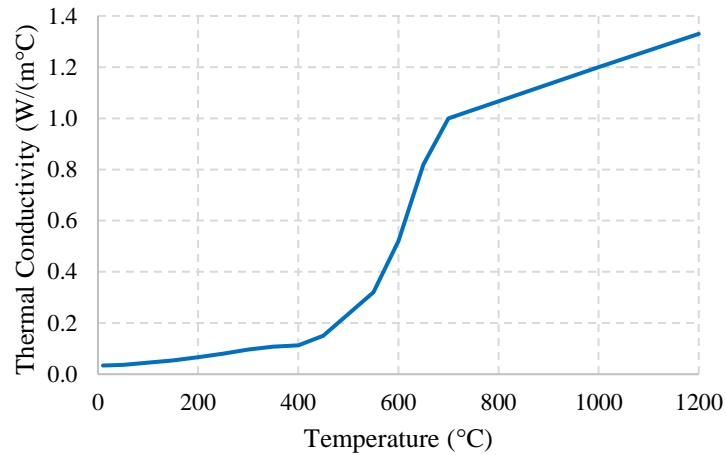
### **2.1 Thermal properties of 3D printed concrete at elevated temperature**

It is important to incorporate elevated temperature material properties for the model since material properties change with the temperature, and each time step, temperature distribution varies with the fire exposure. Moreover, the fire design of 3D printed concrete requires proper knowledge on the elevated temperature thermal properties as the printable concrete mix behaves differently from conventional aggregate concrete. In order to numerically model the thermal behaviour of the structure to precisely predict the FRL, accurate estimation of thermal properties is essential. Hence, thermal conductivity, specific heat, and relative density of the

3D printed concrete with elevated temperature are required. In this study, these temperature-dependent thermal properties obtained from EN 1992-1-2 [62] were used with suitable modification for the specific heat variation within 20-120°C temperature range whilst thermal conductivity and relative density changes followed the conventional concrete behaviour [30]. These revisions were validated against the results of experimental fire test of 3D printed concrete (described in Section 3). Fig 3 illustrates the deemed and proposed thermal properties of 3D printed concrete at higher temperatures. As this analysis covers the impact of cavity insulation on the fire performance of 3D printed concrete non-load bearing wall, thermal properties of the mineral wool material are also explained under this section (Fig 4). For the mineral wool material, the constant density of 80 kg/m<sup>3</sup> and specific heat of 840 J/kg.°C are considered at elevated temperatures [49].



**Fig 3: Thermal properties of 3D printed concrete with increasing temperature: (a) Relative density; (b) Thermal conductivity; (c) Specific heat [30]**



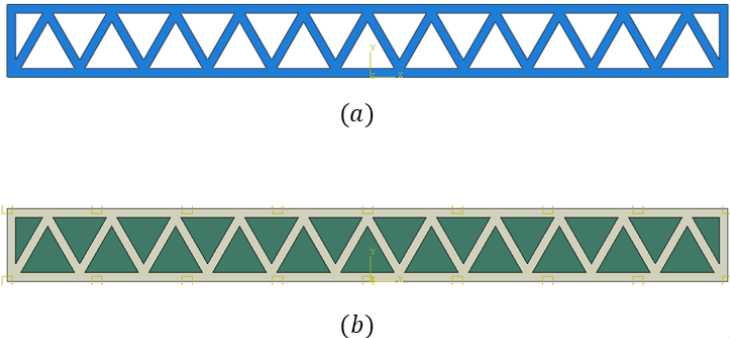
**Fig 4: Thermal conductivity of Mineral wool [49]**

## 2.2 Heat transfer FE model

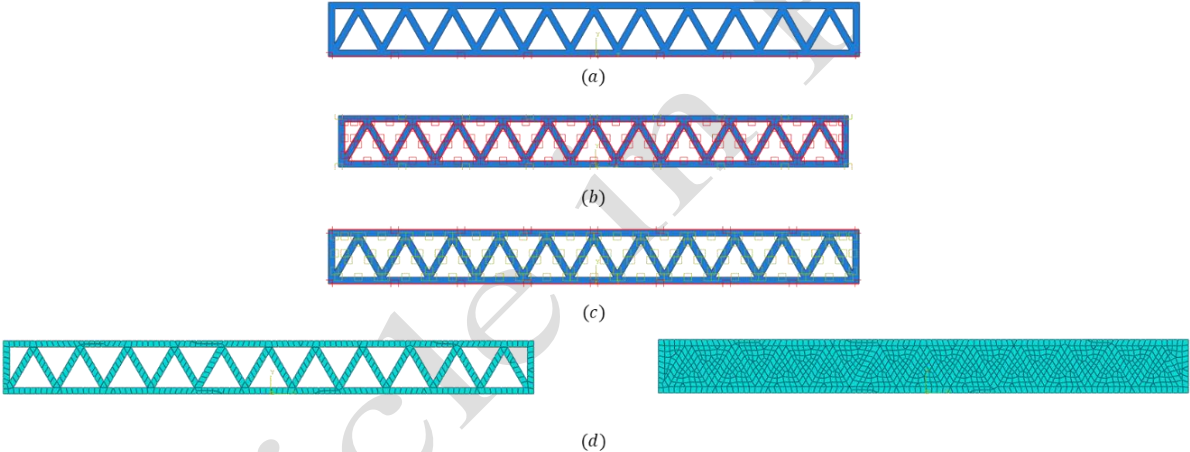
Following steps were conducted in modelling and analysing the 3D printed concrete walls under fire exposure. Initially, the geometry of the model was created. Wall configuration was considered with the cavity, and the same wall configuration was considered when the cavity is filled with mineral wool insulations. Therefore, geometry walls created with the void (cavity) and cavity filling parts were created separately and assembled when the wall filled with insulations were modelled, as shown in Fig 5. Once the geometry is created, material properties were assigned to the geometry.

Heat transfer time step with a time period of 14400 seconds (4 hours) was created to evaluate the insulation fire rating of the walls. Fire exposure was assigned as a temperature boundary condition. Due to convection and radiation, heat loss was incorporated as the emissivity of the 0.7 and convection coefficient of  $25 \text{ W/m}^2 \text{ }^\circ\text{C}$  [30], assigned as interaction properties for the wall exposed and unexposed surfaces. For walls with the cavity, heat transfer through the cavity was modelled considering the heat transfer through radiation. Many studies have concluded that heat transfer in voids is governed by heat transfer through radiation [28, 46, 63]; therefore, the emissivity of 0.7 was assigned to the cavity surfaces and modelled as closed cavities in the geometry [62]. For walls filled with insulation material, tie constraints were assigned between the wall and the filling material to model the perfect connection between the two surfaces in heat transfer. Fig 6 illustrates the Abaqus modelling snapshots of the above-mentioned modelling steps.

Analysis was conducted to the prescribed time period, and temperature distribution of the wall with time was generated. Temperature variation of the unexposed surface of the wall was considered for the determination of insulation fire rating as described.



**Fig 5: Geometry of wall configuration (a) with cavity; (b) with cavity insulation**

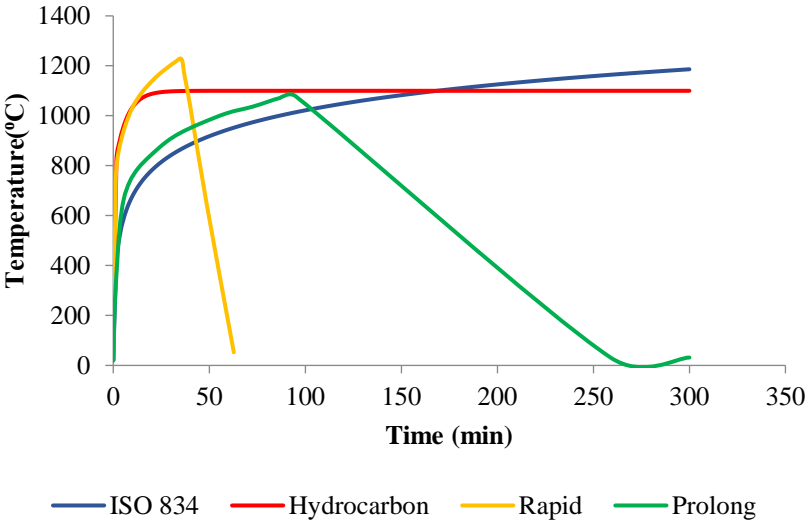


**Fig 6: Abaqus modelling images (a) Boundary condition, (b) Cavity radiation, (c) Surface interaction, (d) Meshing**

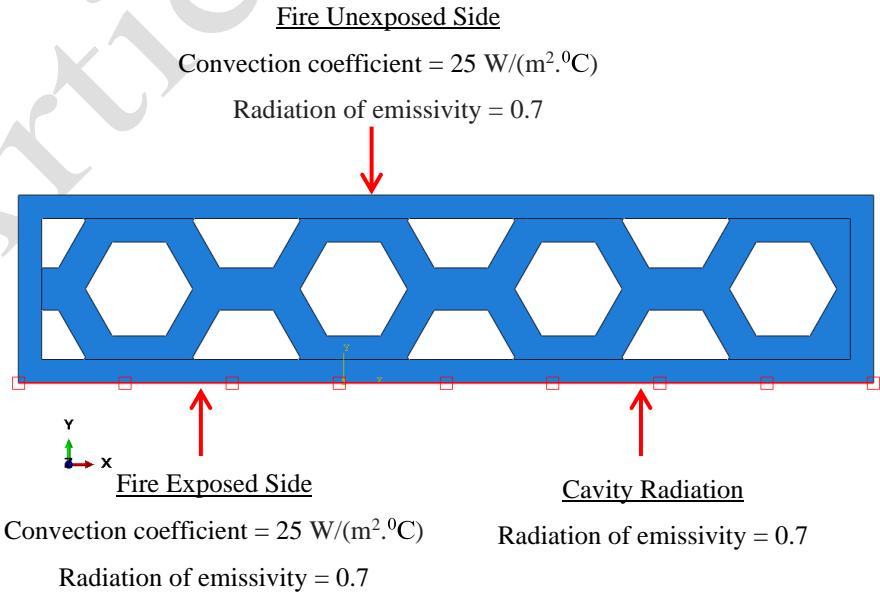
**2.3 Elevated temperature properties variation in a real fire**

Fire exposure can be represented as a temperature variation of the flame with time. This temperature variation with time could be assigned as a boundary condition in fire testing as well as numerical analysis. Fire temperature varies with the fuel load, ventilation characteristics, compartment usage, and openings of the compartment [64-69]. Different standards have defined different time-temperature variations (fire curves), representing fire-induced under different conditions [68]. ISO834 and ASTM E119 are two standard fire curves commonly used. Standard fire curves are used to compare the fire behaviour of structural elements. However, standard fire does not simulate the actual fire situation. The hydrocarbon fire curve is another commonly used fire curved that represents the fire-induced in high fuel loads in fuel sheds and

industrial facilities. Due to the availability of high fuel loads, hydrocarbon fire is more severe than the standard fire. Moreover, parametric fire curves are developed to represent more realistic temperature variations of fire in specific conditions [49, 68, 69]. Eurocode has specified parametric fire curves based on the fuel load, boundary materials, and compartment's opening size. Two parametric fire curves were considered in this study based on the parameters specified in Table 1. Parametric fire contains both heating and decay phases, where standard fire and hydrocarbon fire are considered only the heating phase. Once the burning fuel is burnt off in the actual fire, the fire temperature is lowering, resulting in a decay phase. This realistic situation is accommodated in parametric fire curves. Even in this study's Eurocode parametric fire curves, both the heating and decay phases can be seen (Fig 7).



**Fig 7: Standard fire (ISO 834) and real fire curves**



**Figure 8: Boundary conditions applied on the developed model**

The developed FE model considers fire exposure as a time-temperature variation boundary condition, and elevated temperature material properties are incorporated into the model to achieve accurate results. These thermal properties are assigned to the model as temperature-dependent properties, as shown in Fig 8. However, when the parametric fire is considered, these properties are valid only for the heating phase. During the rapid-fire exposure, the wall undergoes a temperature variation of ambient to 1200 °C in the heating phase and 1200°C to 52°C temperature reduction in the decay phase. Therefore, if only temperature-dependent properties were accommodated, 3D printed concrete wall density would decrease from 2400 kg/m<sup>3</sup> to 2200 kg/m<sup>3</sup> in the heating phase. Again, density would be increased to 2400 kg/m<sup>3</sup> in the decay phase. But it is evident that during the fire exposure, a mass gain cannot happen in the wall. Therefore, thermal properties need to depend on the temperature and the fire phase (heating or decay) to simulate more realistic fire behaviour of walls during the parametric fire exposure.

Temperature plus phase-dependent thermal properties were incorporated in the FE modelling using the subroutine USDFLD. Thermal conductivity, specific heat, and each material's density were assigned as field-dependent properties in the ABAQUS interface. Fortran code was developed to check the temperature and the phase of the fire for each element in each time step and based on both conditions, select the appropriate properties. For instant, during the rapid-fire exposure, 3D printed concrete density would change from 2400 kg/m<sup>3</sup> to 2200 kg/m<sup>3</sup> in the heating phase, and 2200 kg/m<sup>3</sup> remains in the decay phase. These ABAQUS model with subroutine was considered for all the wall configurations to analyse their behaviour in parametric fire conditions.

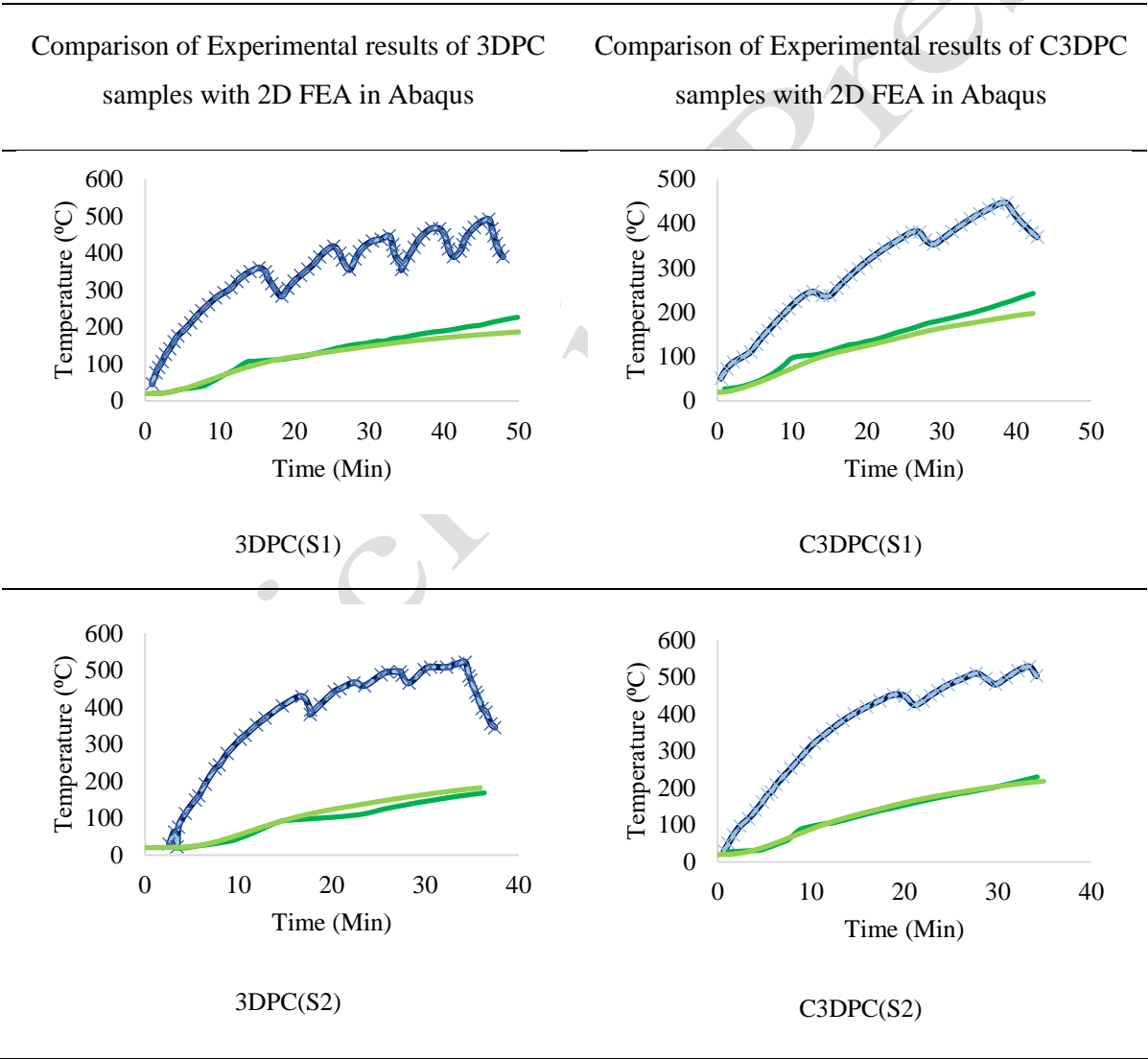
**Table 1: Parametric Fire Curves**

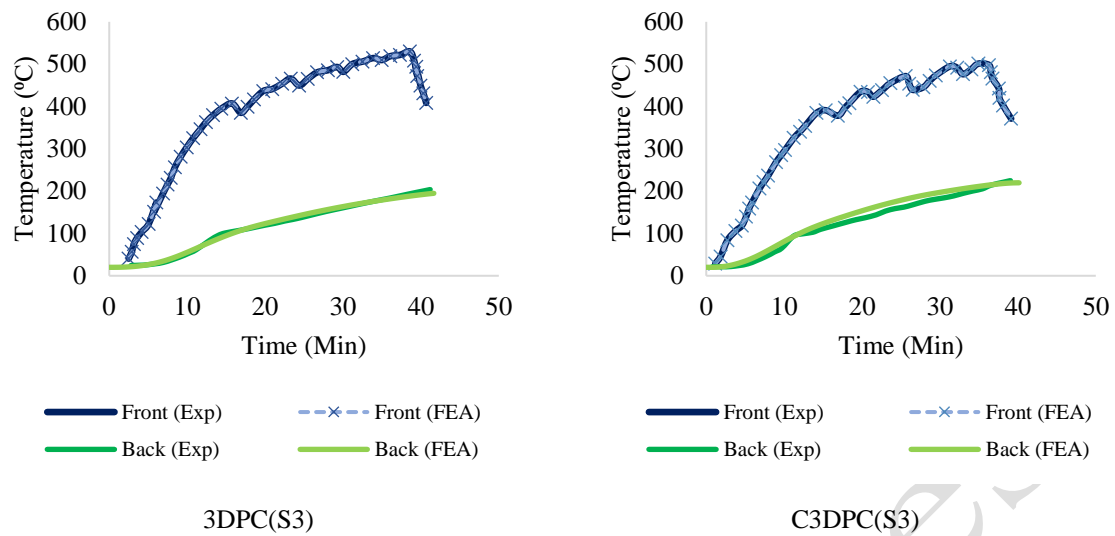
Fire Curve	Rapid Fire	Prolonged Fire
Opening Factor (m <sup>1/2</sup> )	0.08	0.03
Area of Ventilation (m <sup>2</sup> )	2.85	1.44
Compartment thermal Inertia (J/m <sup>2</sup> S <sup>1/2</sup> K)	715	702

### 3. Validation

Validation of a numerical FE model is a process of authentication of the exactitude of the models in terms of presumed revisions and the material characterization associated with the existing experimental results. For the validation procedure, the study by Cicione et al. [53] is used, in which the performance of 3D printed concrete at elevated temperatures was investigated experimentally. The fire test results from this study which has been obtained for three 3D printed concrete (3DPC) panels of 160×165×50 mm and three 3D printed and cut samples (C3DPC) of 160×160×40 mm were used for this FE model validation.

**Table 2: 2D FEA Validation of 3DPC and C3CPD Samples [30]**





The detailed validation has been conducted by authors previously for heat transfer FE models in 2D and 3D using ABAQUS [61] and also 2D heat transfer FE models using MATLAB. The created FE models were verified against the findings acquired from the existing experimental study [30]. The unexposed surface temperature of experimental curves and FEA curves showed excellent agreement. Since the time-temperature variation results are nearly identical, it could be assumed that the revised thermal properties identified for the 3D printed concrete could be applied for parametric study of fire performance of 3D printed concrete walls. Since, this study is concentrated on 2D analysis, the evaluation of experimental results with 2D FEA in ABAQUS is presented in Table 2 for 3DPC samples and C3DPC samples, correspondingly.








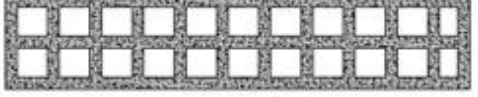



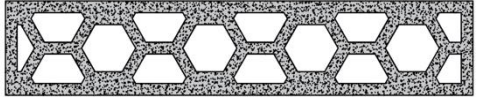
#### 4. Parametric Study of 3D printed concrete wall section specimens

This section covers the parametric study to obtain the insulation fire ratings of non-load bearing 3D printed concrete wall panels with biomimetic hollow cross sections under realistic fire curves using the validated FE model. The time needed for the unexposed surface to become 160°C is quantified as the insulation fire rating of these wall panels. From the previous study by authors [30], it was found that the insulation fire rating is rising with the rise in density regardless of the wall thickness. Hence the printable concrete with density of 2400 kg/m<sup>3</sup> has been selected in this study for further analysis. Six (6) 3D printed concrete wall panels with biomimetic hollow cross sections (C1, C2, C3, C4, C5 and C6) and those wall panels were then combined with the Mineral wool cavity insulation to enhance the fire behaviour (CI1, CI2, CI3, CI4, CI5 and CI6) were involved in this study. Consequently, the model was expanded to study 96, 3D printed wall specimens against several parameters such as, wall thickness (100 mm and 200mm) and six different wall structures with and without cavity insulation. In this study, heat



transfer analysis was performed on wall panels with thicknesses of 100 mm (12 mm layer thickness) and wall thicknesses of 200 mm (25 mm layer thickness). The nozzle sizes were chosen based on the real constructed structures. The different wall panels with biomimetic hollow cross sections are shown in Table 3 and the same wall panels were examined with mineral wool cavity insulation. The detailed parametric study outline is presented in Table 4.

**Table 3: Different cross-sectioned 3D printed concrete wall configurations**

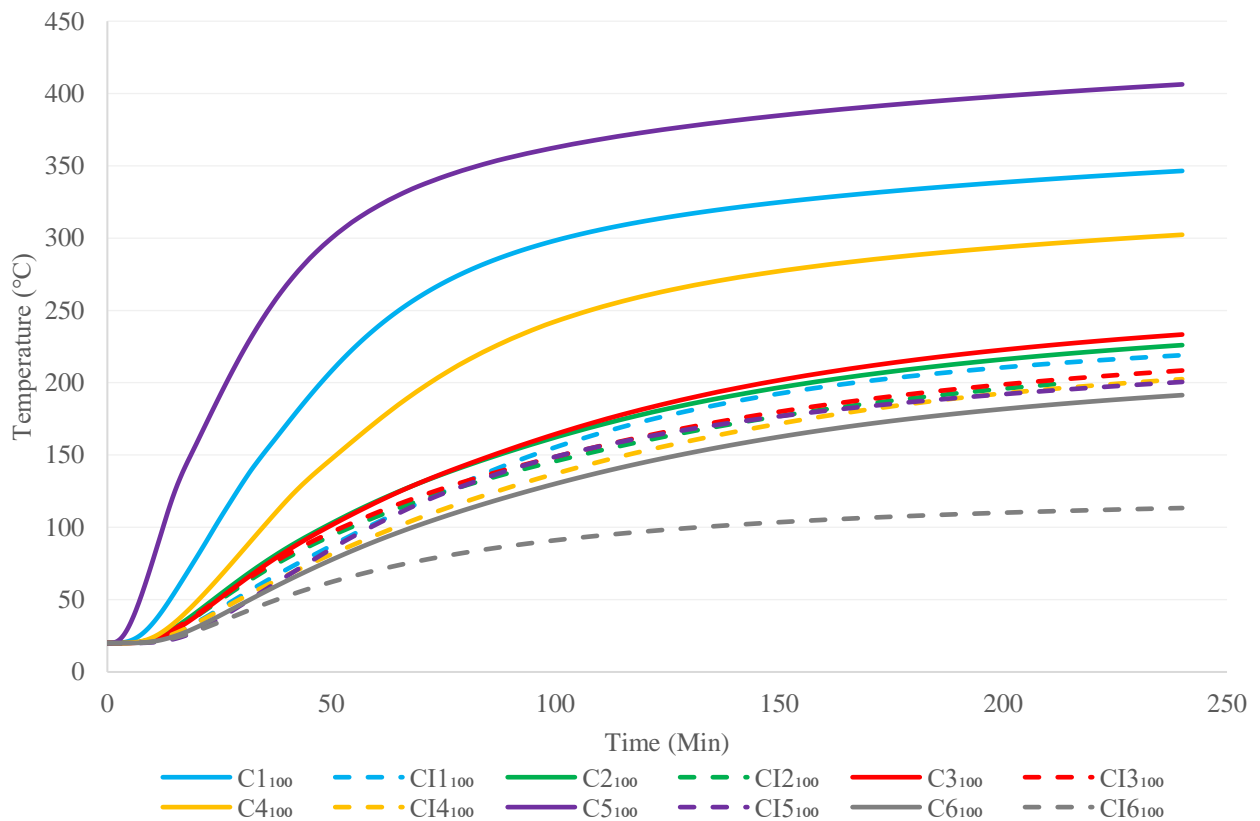
Wall Configuration (1 m length)	100 mm (12 mm layer)	200 mm (25 mm layer)
C1 Truss		
C2 Triangular		
C3 Triangular		
C4 Lattice		
C5 Lattice		
C6 Cellular		

**Table 4: Outline of Parametric Study**

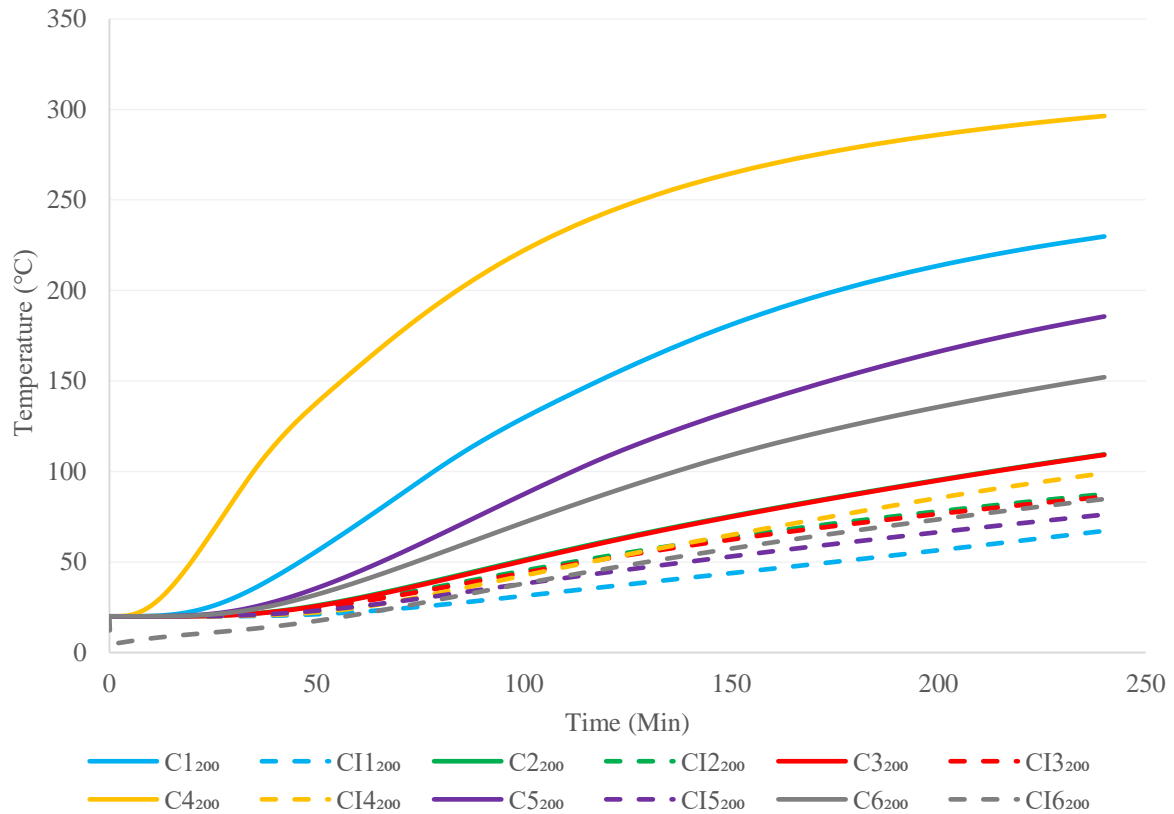
Fire Scenario	Density (kg/m <sup>3</sup> )	Thickness of the wall (mm)	Wall configuration	Models
ISO Fire	2400	100	C1, C2, C3, C4, C5, C6	24
		200	CI1, CI2, CI3, CI4, CI5, CI6	
Hydrocarbon	2400	100	C1, C2, C3, C4, C5, C6	24
		200	CI1, CI2, CI3, CI4, CI5, CI6	
Rapid Fire	2400	100	C1, C2, C3, C4, C5, C6	24
		200	CI1, CI2, CI3, CI4, CI5, CI6	
Prolonged Fire	2400	100	C1, C2, C3, C4, C5, C6	24
		200	CI1, CI2, CI3, CI4, CI5, CI6	
Total				96

## 5. Results and Discussion

### 5.1 Standard Fire



**Figure 9(a): Unexposed Surface temperature variation of 100 mm wall configurations subjected to Standard fire**



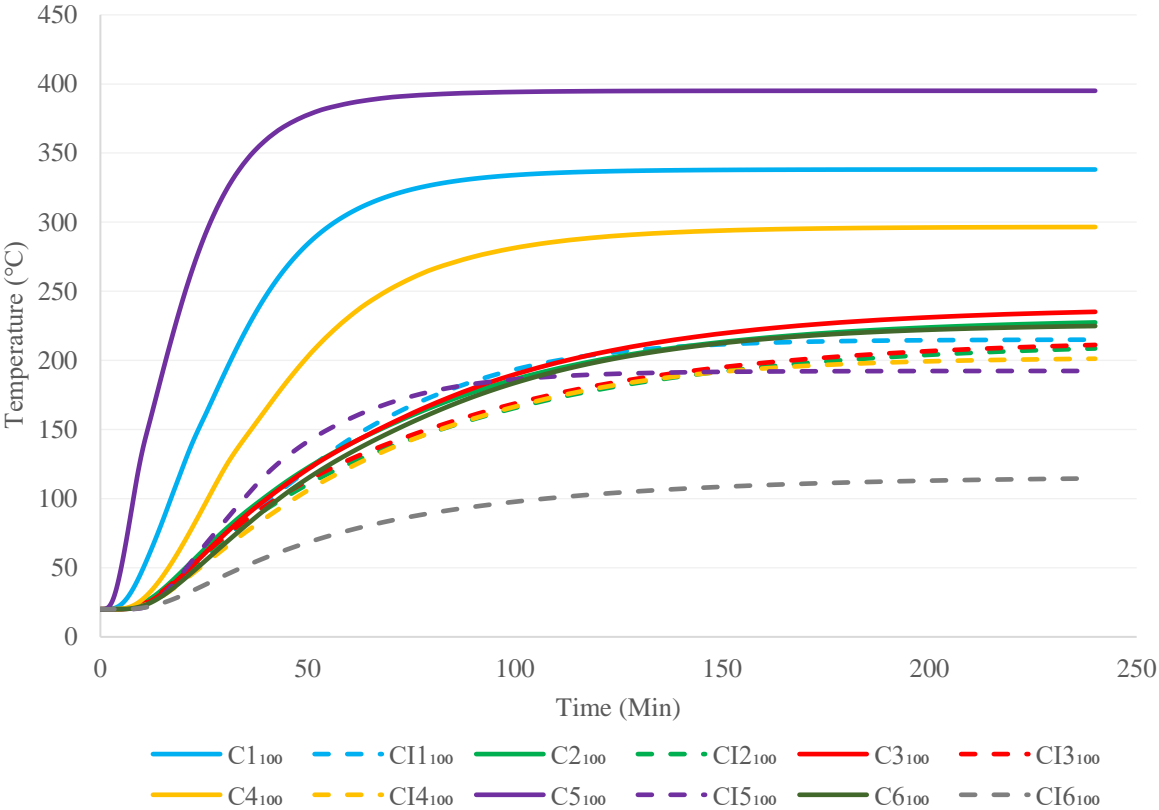
**Figure 9(b): Unexposed Surface temperature variation of 200 mm wall configurations subjected to Standard fire**

Figure 9 (a & b) illustrate the unexposed surface temperature-time history of different 3D printed concrete walls subjected to standard fire with 100mm and 200mm thickness, respectively. The temperature increment in the unexposed surface of the 100mm wall panels is remarkably higher at the early time, whereas gentler temperature rises at the latter stage. However, the 200mm thickness wall panels showed relatively lower temperature rise at the beginning compared to 100 mm walls, hence showed better fire performance with a higher insulation fire rating at most of the cases. Therefore, it could be concluded that the increase in wall thickness result in enhanced fire performance. In terms of different cross-sectional configurations, C6 cellular cross sectional wall panel exhibited superior fire performance compared to other wall panels with and without mineral wool insulation. Moreover, C2 and C3 double row wall panels with triangular sections showed enhanced fire performance compared to the other C1 and C5 single row wall panels with truss and lattice sections for both 100mm and 200mm wall panels. The introduction of higher intermediate barriers could be found as the reason for the reduction on material conductivities; hence improved insulation fire rating has been obtained. In contrast, C4 wall configuration with double row lattice arrangement showed somewhat similar behaviour regardless the wall thickness. Moreover, it is obvious that the

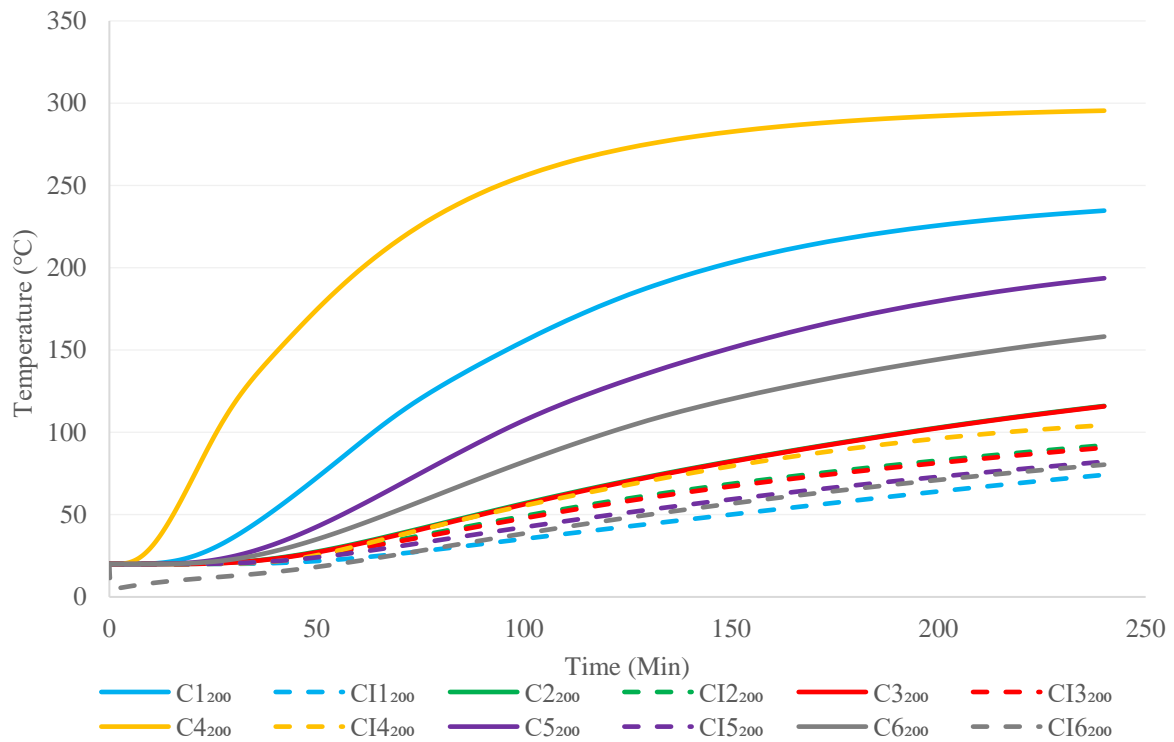
mineral wool infilled cavity walls resulted in improved fire performance with lower temperature at the unexposed surface than that of cavity walls irrespective of the cross-sectional arrangements and wall thickness. C6 cellular cross sectional wall panel showed the highest performance under fire among 100 mm walls, and CI1 truss cross sectional wall exhibited the highest performance under fire among 200 mm with mineral wool cavity insulation.

**5.2 Hydrocarbon Fire**

The time-temperature change of the unexposed side of the 3D printed concrete wall panels under hydrocarbon fire condition with 100mm and 200mm wall thickness are presented in Figure 10 (a & b). Similarly standard fire, a higher temperature increase has been observed for the unexposed surface at early stage for 100 mm wall panels and comparatively lesser increment for 200 mm walls. Hydrocarbon fire case resulted in nearly related behaviour of time-temperature profiles of standard fire for all the different cross sections. CI6 cellular cross sectional wall panel presented the higher performance among 100 mm walls and CI1 truss cross sectional wall exhibited the higher performance under fire among 200 mm with mineral wool cavity insulation. Moreover, the unexposed surface temperature has reached a persistent value over time at later phases due to the nature of hydrocarbon fire response.

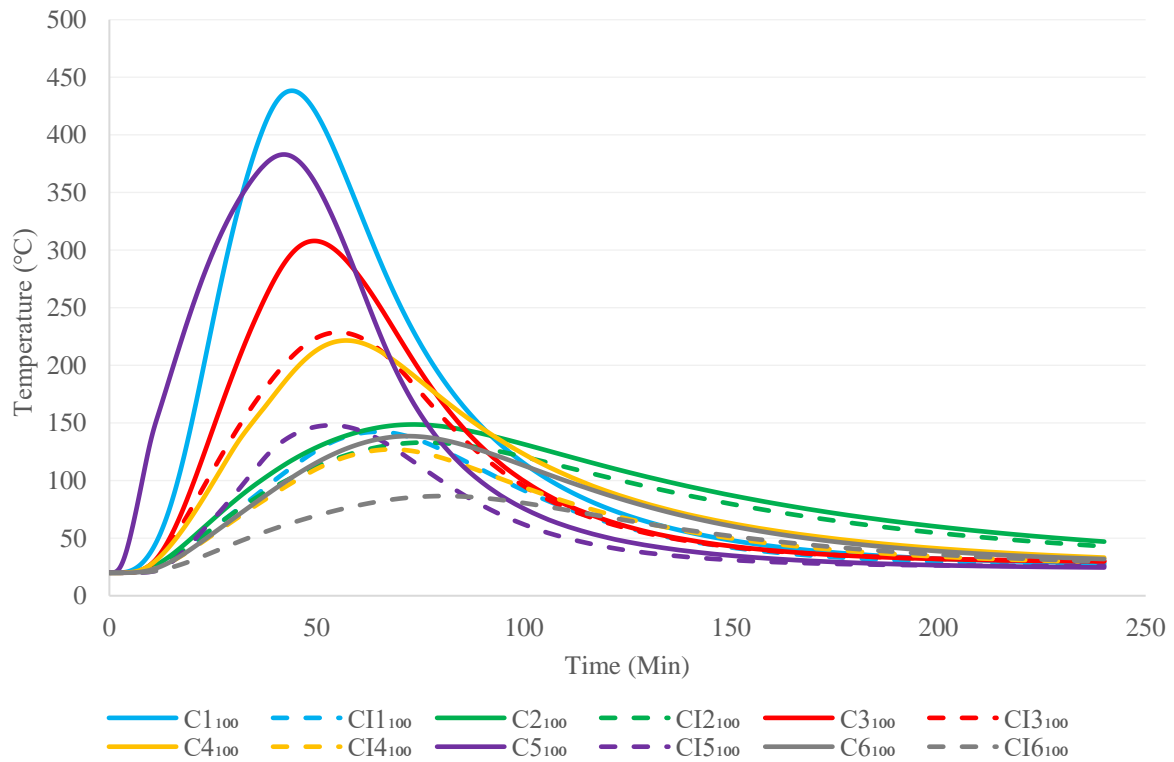


**Figure 10(a): Unexposed Surface temperature variation of 100 mm wall configurations subjected to Hydrocarbon fire**

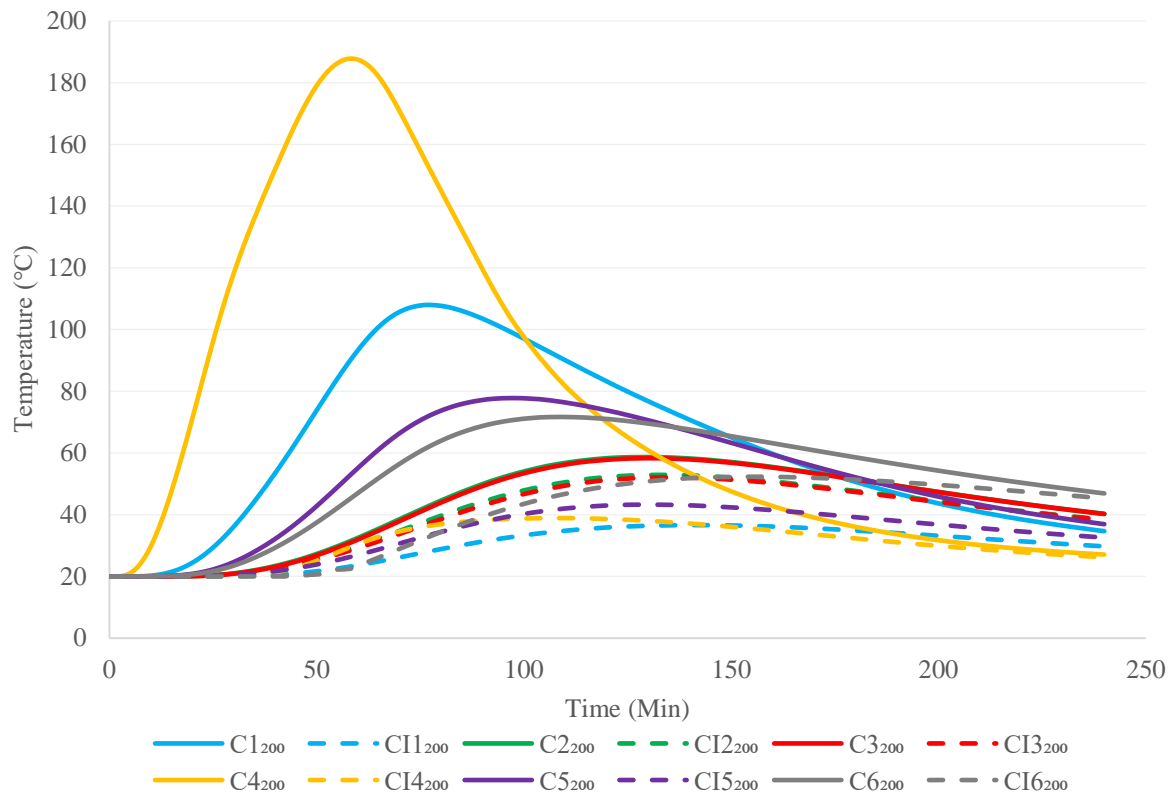


**Figure 10(b): Unexposed Surface temperature variation of 200 mm wall configurations subjected to Hydrocarbon fire**

### 5.3 Rapid Fire



**Figure 11(a): Unexposed Surface temperature variation of 100 mm wall configurations subjected to Rapid fire**

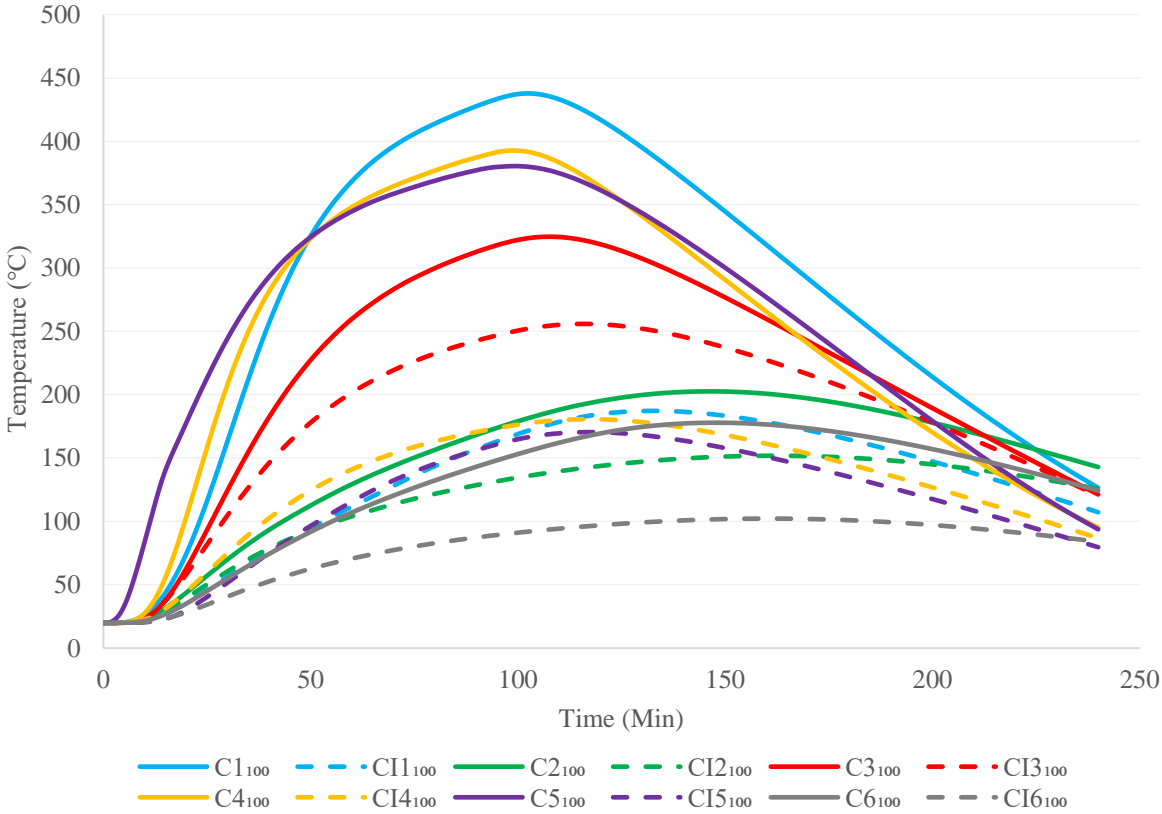


**Figure 11(b): Unexposed Surface temperature variation of 200 mm wall configurations subjected to Rapid fire**

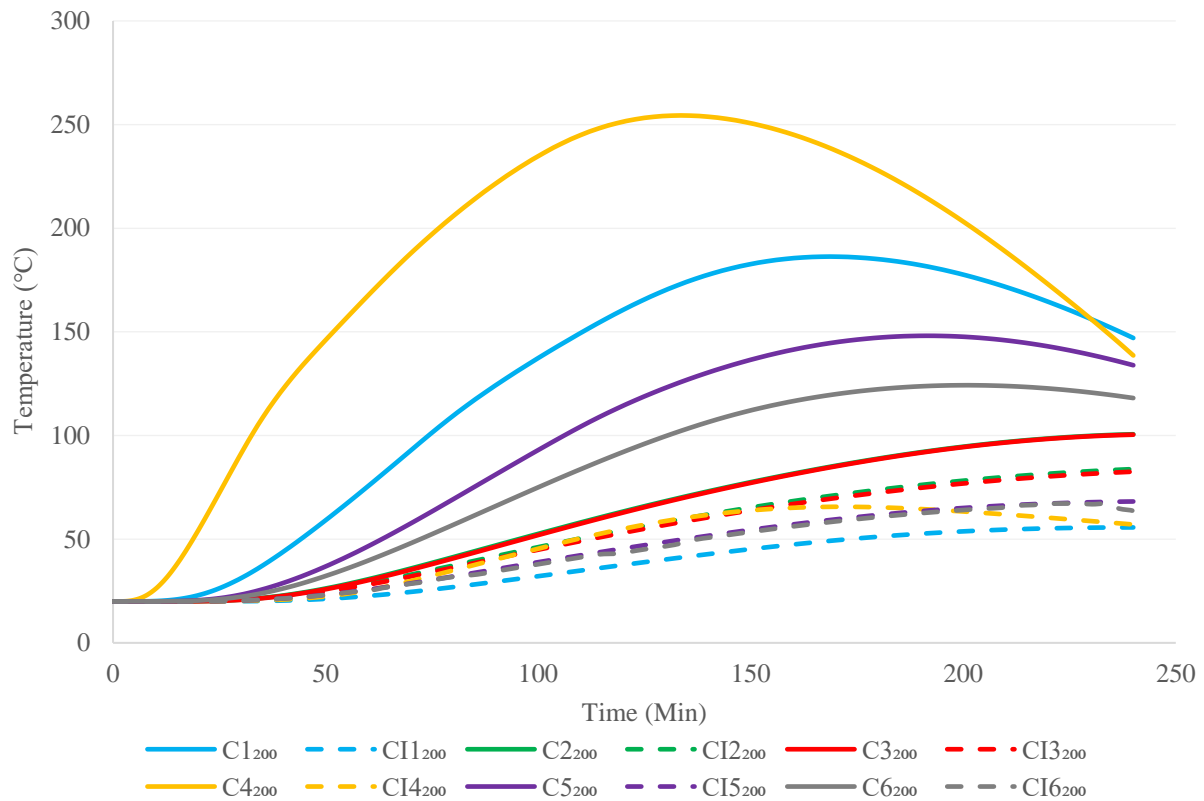
The time-temperature change of the 3D printed concrete wall panels on the unexposed side under rapid fire situation is shown in Figures 11 (a & b). The impact of rapid fire is identified as critical through the earliest 1-hour time duration, resulting in rapid temperature increment. Afterwards, since the real fire curve maintains a decline phase, a considerable temperature reduction has been found. The rapid-fire situation revealed the lower fire resistance rate for the cavity wall configurations with 100 mm thickness single row arrangement, hence with higher severity contrasted to the other three fire conditions. However, among the 100mm wall panels triangular sectional wall C3 and amongst the 200mm walls C4 with double lattice row arrangement showed irregular variation. These contradictory observations must be further investigated. Furthermore, it should be remarked that both the cavity C2 triangular wall and C6 cellular wall have not achieved the insulation failure fire rating temperature of 160°C within the 4 hours of rapid-fire contact. Similarly, for the 200mm wall panels, insulation failure has not discovered apart from the cavity wall panel C4. It is evident that the mineral wool infilled cavity walls resulted in improved fire performance than that of cavity walls regardless of the cross-sectional arrangements and wall thickness.

### 5.4 Prolonged Fire

Figures 12 (a & b) illustrate the unexposed surface temperature-time change of 3D printed concrete walls exposed to prolong fire condition. The temperature increase is notably greater at the early 2-hour period and observed by a temperature drop at the latter stages. It demonstrates moderately better insulation fire rating compared to hydrocarbon and rapid fire whilst indicated a reduced value associated to standard fire situation as expected. Prolonged fire scenario ensued in nearly similar performance of time-temperature profiles of rapid fire for all the different cross sections. CI6 cellular and CI1 truss wall panels displayed the higher performance under fire among 100 mm and 200mm respectively with mineral wool cavity insulation. It is notable that the C2, C3, C5 and C6 cavity walls with 200mm thickness have not attained the temperature of 160°C within the 4 hours. Also, for all the 200mm mineral wool insulated wall panels no insulation failure has been detected.



**Figure 12(a): Unexposed Surface temperature variation of 100 mm wall configurations subjected to Prolonged fire**



**Figure 12(b): Unexposed Surface temperature variation of 200 mm wall configurations subjected to Prolonged fire**

### 5.5 Effect of individual real fire on different wall configurations

The insulation fire rating of the wall configurations obtained from the produced time-temperature outlines under real fire circumstances are presented in Tables 5 and 6. The results explain that moderately same fire resisting time has been achieved for standard and prolong fire situations whilst fire resisting time for hydrocarbon and rapid fire also quite similar. This shows that the attributes of the fire curves with the maximum fire temperature and the subsequent time, and the rate of reduction considerably inspired the unexposed temperature of 3D printed concrete walls. Moreover, for the wall panels with single row configurations showed superior fire performance when mineral wool insulation has been incorporated (Fig 14). However, the double row configurations have shown lesser enhancement in the fire performance with insulation irrespective of the cross-sectional arrangements (Fig 13). These phenomena can be explained as the void area is much large in those walls, the cavity radiation effect and the impact of insulation is different.

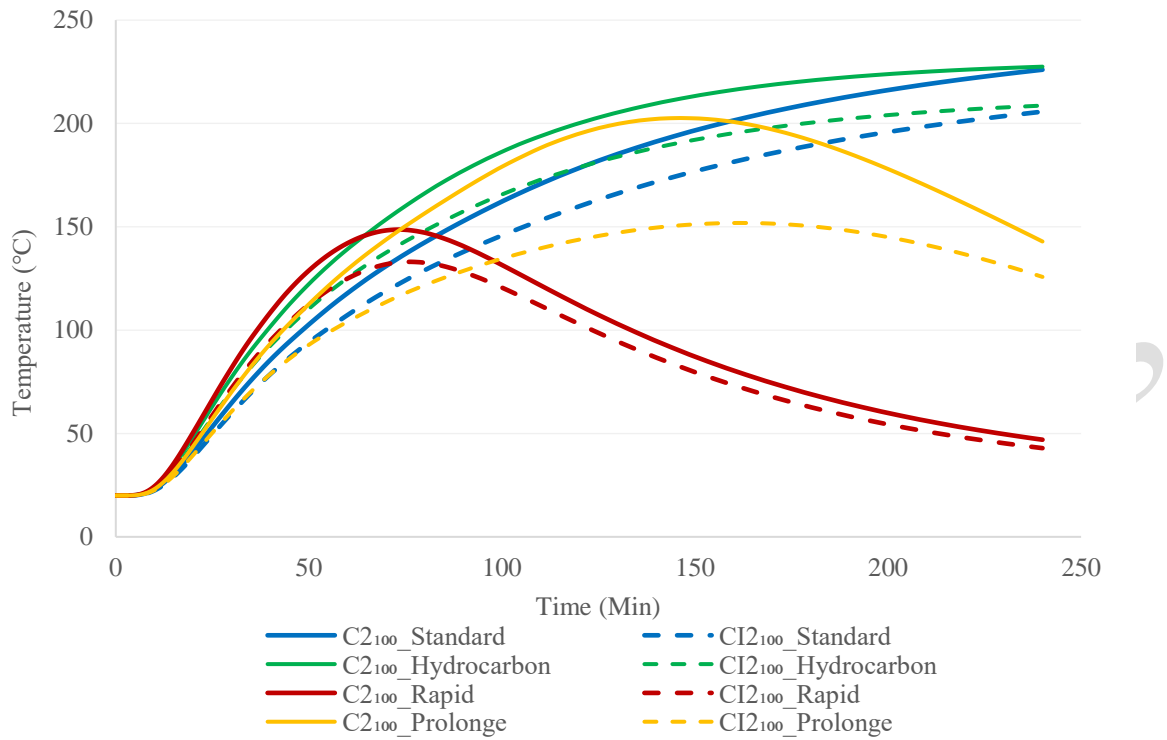


**Table 5: Insulation fire ratings for 3D printed concrete walls (100 mm series)**

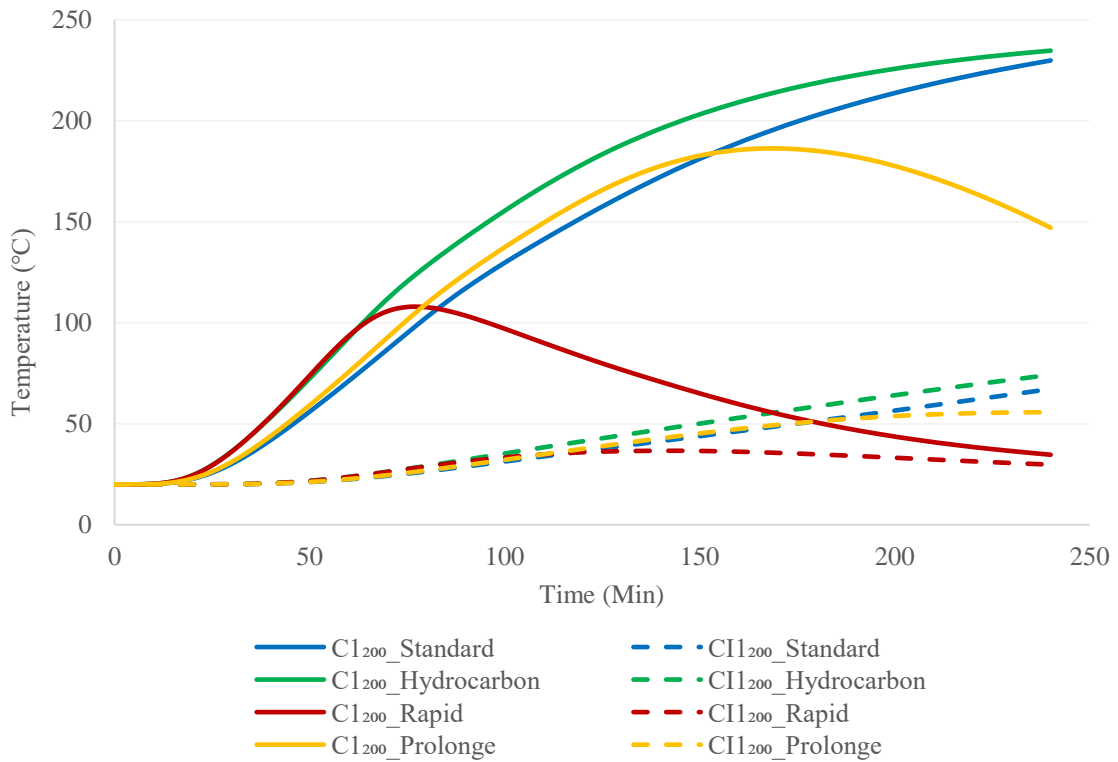
Configurations		Insulation failure time under different fire exposure (mins)			
		Standard fire	Hydrocarbon fire	Rapid fire	Prolonged fire
Cavity walls	C1 <sub>100</sub>	37	25	20	29
	C2 <sub>100</sub>	97	75	-	82
	C3 <sub>100</sub>	95	74	27	35
	C4 <sub>100</sub>	53	38	36	25
	C5 <sub>100</sub>	20	12	12	17
	C6 <sub>100</sub>	144	78	-	106
Mineral wool infilled walls	CI1 <sub>100</sub>	104	70	-	92
	CI2 <sub>100</sub>	120	93	-	-
	CI3 <sub>100</sub>	116	89	33	44
	CI4 <sub>100</sub>	128	91	-	76
	CI5 <sub>100</sub>	112	61	-	94
	CI6 <sub>100</sub>	-	-	-	-

**Table 6: Insulation fire ratings for 3D printed concrete cavity walls (200 mm series)**

Configurations		Insulation failure time under different fire exposure (mins)			
		Standard fire	Hydrocarbon fire	Rapid fire	Prolonged fire
Cavity walls	C1 <sub>200</sub>	125	101	-	119
	C2 <sub>200</sub>	-	-	-	-
	C3 <sub>200</sub>	-	-	-	-
	C4 <sub>200</sub>	60	44	42	56
	C5 <sub>200</sub>	187	159	-	-
	C6 <sub>200</sub>	-	-	-	-



**Figure 13: Unexposed Surface temperature change of 100mm wall configurations C2 and CI2 under different fire conditions**



**Figure 14: Unexposed Surface temperature change of 200mm wall configurations C1 and CI1 under different fire conditions**

Figures 15 (a-d) illustrate the temperature distribution obtained from finite element analysis for cellular cross sectional wall configurations (C6) after 4 hrs of heat transfer under considered fire scenarios. Non-uniform temperature distribution can be observed due to the integration of insulation material. Moreover, the severity of rapid fire and prolonged fire on the wall panels compared to standard and hydrocarbon fire curves could be observed clearly through this temperature distribution.

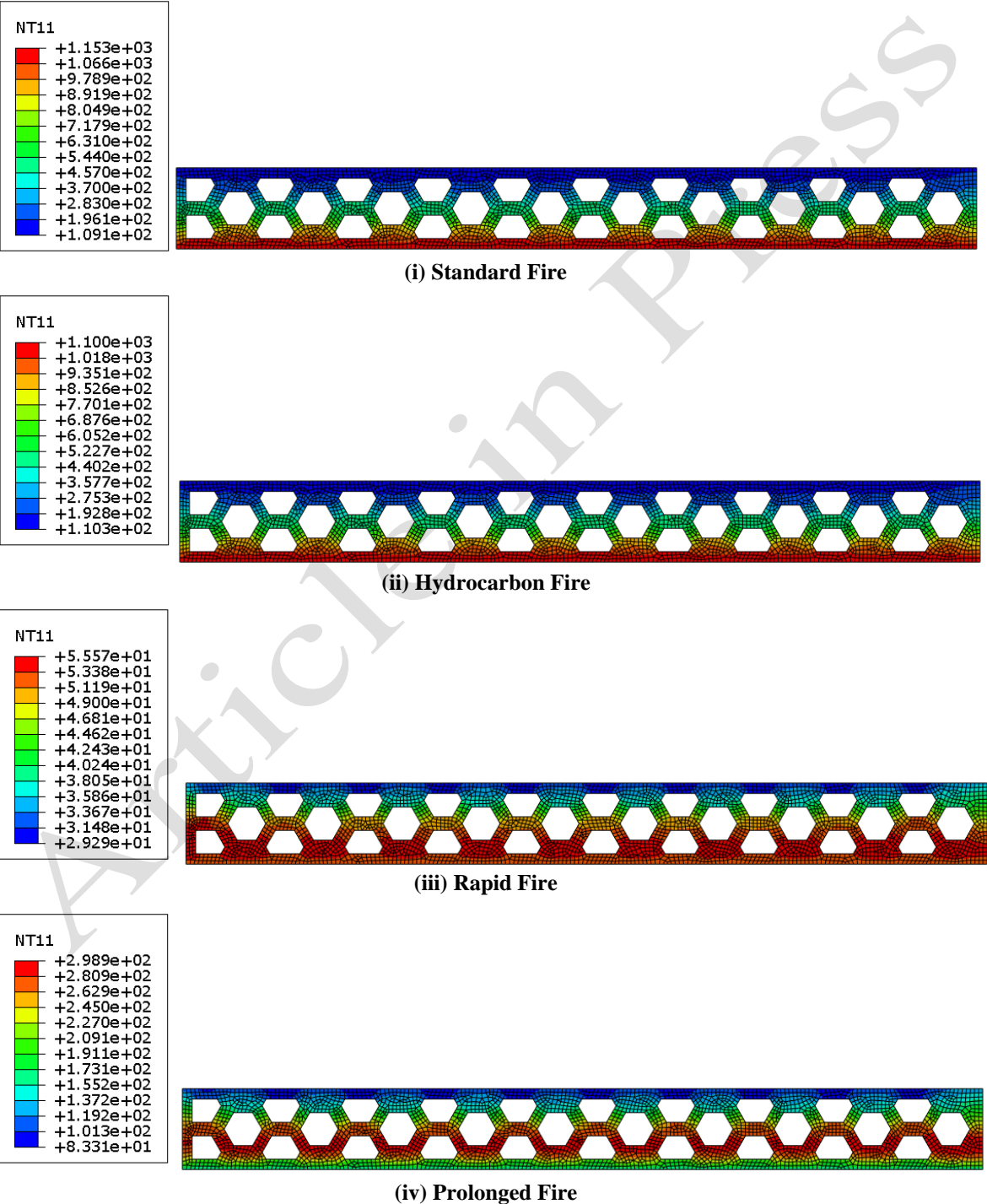
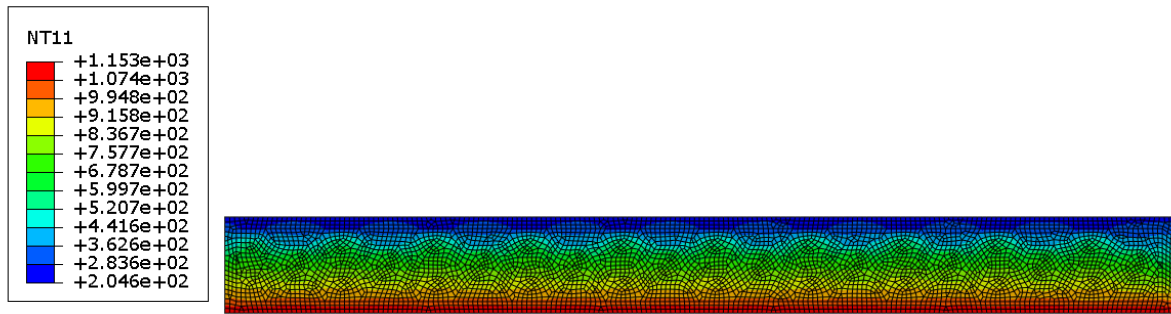
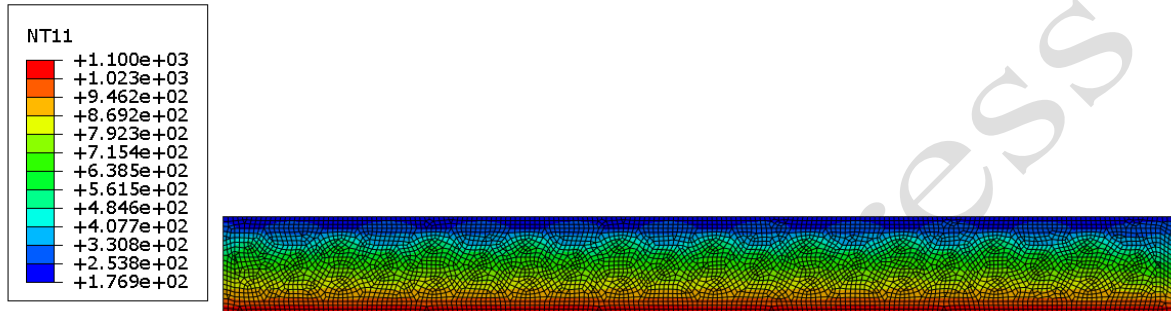


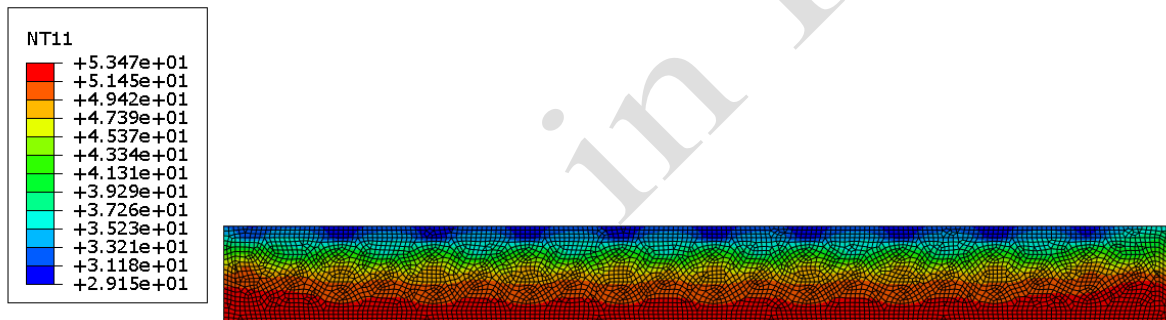
Figure 15(a): Temperature distribution of C6100 wall panel



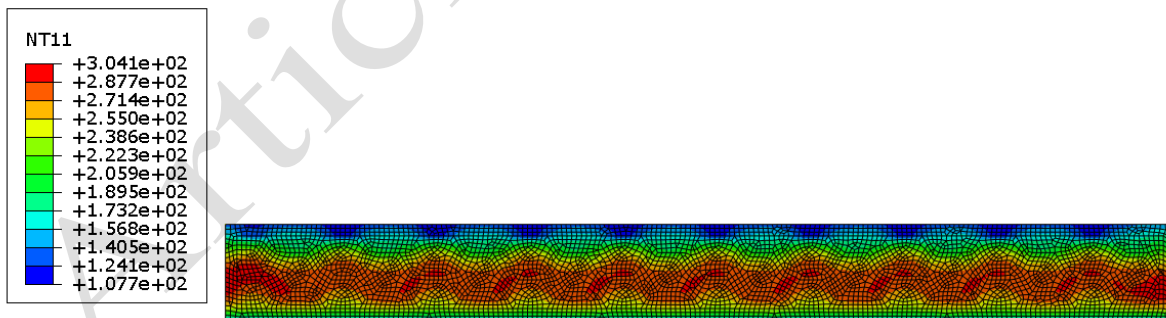
(i) Standard Fire



(ii) Hydrocarbon Fire

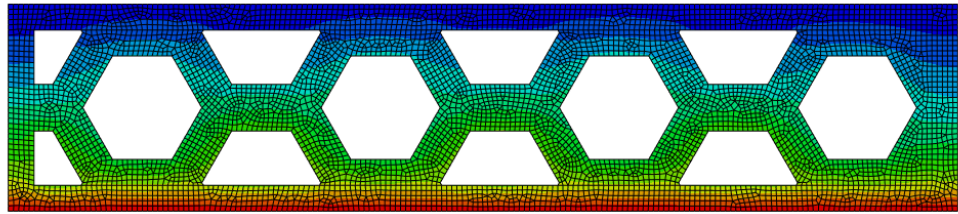
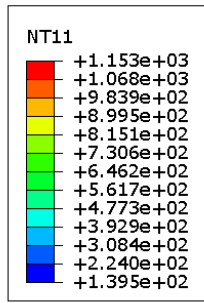


(iii) Rapid Fire

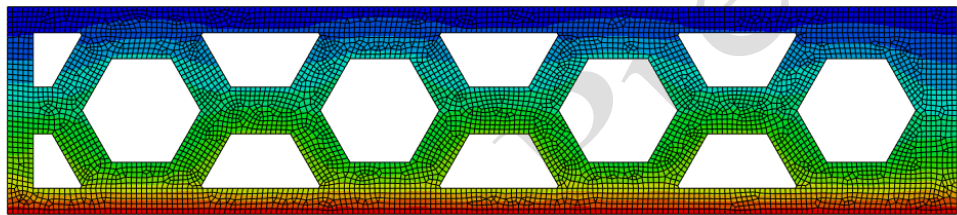
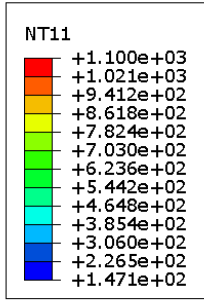


(iv) Prolonged Fire

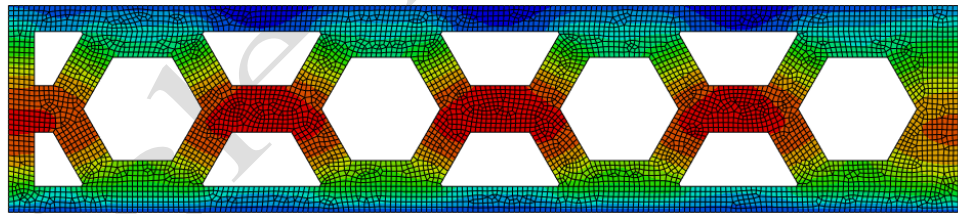
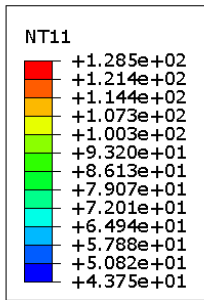
Figure 15(b): Temperature distribution of CI6<sub>100</sub> wall panel



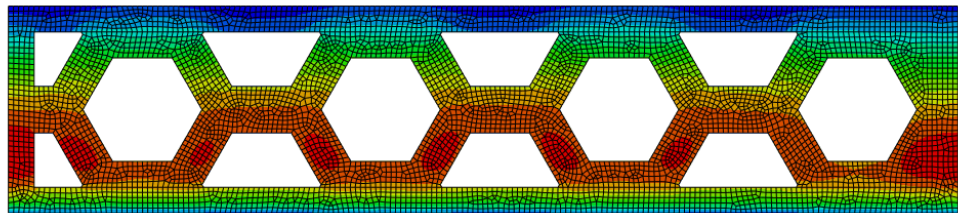
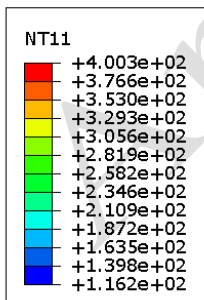
(i) Standard Fire



(ii) Hydrocarbon Fire



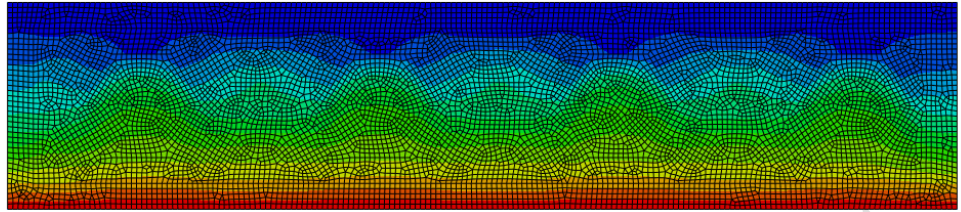
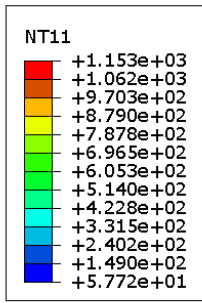
(iii) Rapid Fire



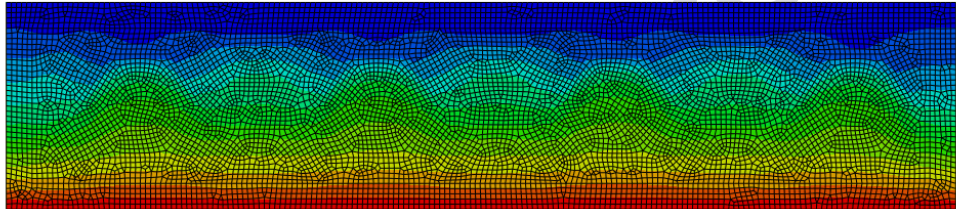
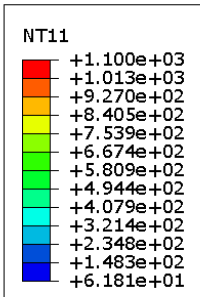
(iv) Prolonged Fire

Figure 15(c): Temperature distribution of C6<sub>200</sub> wall panel

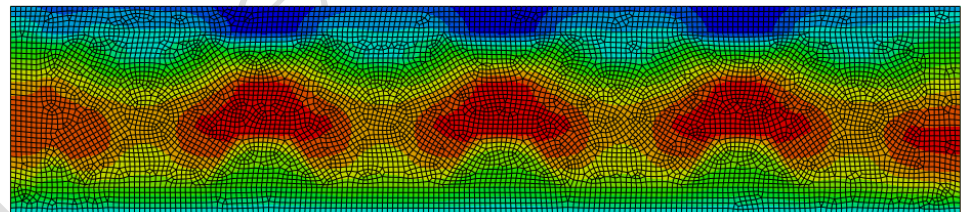
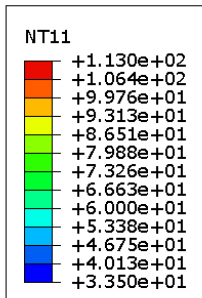




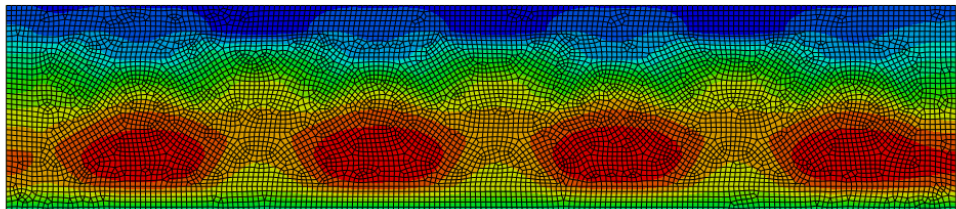
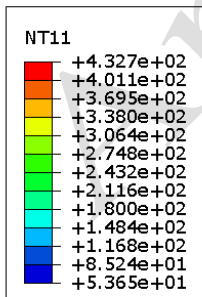
(i) Standard Fire



(ii) Hydrocarbon Fire



(iii) Rapid Fire



(iv) Prolonged Fire

Figure 15(d): Temperature contours of CI6<sub>200</sub> wall panel

## 6. Conclusion

Research in 3DCP is primarily concentrated on materials, automation and structural strength, there are still many characteristics related to the fire behaviour and thermal efficiency that need further study. Furthermore, the numerical simulation of the 3DCP method is a quite new research area in dynamic growth with many questions remaining. Therefore, this paper has presented the findings of numerical studies on the fire performance of bio inspired 3D printed concrete walls that involved both the cavity walls and cavity insulated wall configurations. The effect of wall thickness, cross sectional arrangements and cavity insulation on the Insulation Fire rating under different realistic fire scenarios were examined. Finally, several conclusions can be described as follows:

- Non-load bearing 3D printed concrete cavity walls showed lesser insulation failure fire rating, whereas 3D printed concrete cavity walls insulated with mineral wool resulted in an excellent fire rating.
- The individual fire curves considerably affect the unexposed surface temperature increase of wall panels. The outcomes prove that rapid fire and prolonged fire are crucial on the fire performance associated to standard and hydrocarbon fire curves.
- Ample enhancement on fire performance was observed when the wall thickness of 3D printed concrete walls is increased from 100mm to 200mm.
- The cellular configuration (C6) has shown greater fire performance with mineral wool insulation compared to other wall configurations regardless the fire scenario.
- The fluctuating fire behaviour of these wall configurations has to be investigated further considering the measured thermal properties of 3D printable concrete at higher temperatures and with the incorporation of structural failures.

## Reference

- [1] B. Furet, P. Poullain, and S. Garnier, "3D printing for construction based on a complex wall of polymer-foam and concrete," *Additive Manufacturing*, vol. 28, pp. 58-64, 2019, doi: 10.1016/j.addma.2019.04.002.
- [2] M. Adaloudis and J. Bonnin Roca, "Sustainability tradeoffs in the adoption of 3D Concrete Printing in the construction industry," *Journal of Cleaner Production*, vol. 307, 2021, doi: 10.1016/j.jclepro.2021.127201.
- [3] M. S. Khan, F. Sanchez, and H. Zhou, "3-D printing of concrete: Beyond horizons," *Cement and Concrete Research*, vol. 133, 2020, doi: 10.1016/j.cemconres.2020.106070.
- [4] J. Xiao *et al.*, "Large-scale 3D printing concrete technology: Current status and future opportunities," *Cement and Concrete Composites*, vol. 122, 2021, doi: 10.1016/j.cemconcomp.2021.104115.
- [5] S. Pessoa, A. S. Guimarães, S. S. Lucas, and N. Simões, "3D printing in the construction industry - A systematic review of the thermal performance in buildings," *Renewable and Sustainable Energy Reviews*, vol. 141, 2021, doi: 10.1016/j.rser.2021.110794.
- [6] C. Menna *et al.*, "Opportunities and challenges for structural engineering of digitally fabricated concrete," *Cement and Concrete Research*, vol. 133, 2020, doi: 10.1016/j.cemconres.2020.106079.
- [7] S. A. Khan, M. Koç, and S. G. Al-Ghamdi, "Sustainability assessment, potentials and challenges of 3D printed concrete structures: A systematic review for built environmental applications," *Journal of Cleaner Production*, vol. 303, 2021, doi: 10.1016/j.jclepro.2021.127027.
- [8] T. Ooms, G. Vantghem, R. Van Coile, and W. De Corte, "A parametric modelling strategy for the numerical simulation of 3D concrete printing with complex geometries," *Additive Manufacturing*, vol. 38, 2021, doi: 10.1016/j.addma.2020.101743.
- [9] V. Mechtcherine *et al.*, "Extrusion-based additive manufacturing with cement-based materials – Production steps, processes, and their underlying physics: A review," *Cement and Concrete Research*, vol. 132, 2020, doi: 10.1016/j.cemconres.2020.106037.
- [10] S. C. Paul, G. P. A. G. van Zijl, M. J. Tan, and I. Gibson, "A review of 3D concrete printing systems and materials properties: current status and future research prospects," *Rapid Prototyping Journal*, vol. 24, no. 4, pp. 784-798, 2018, doi: 10.1108/rpj-09-2016-0154.
- [11] B. Yazyev, E. Karpova, G. Skripkiunas, A. Sedova, and Y. Tsimbalyuk, "Additive manufacturing of concrete wall structures," *E3S Web of Conferences*, vol. 281, 2021, doi: 10.1051/e3sconf/202128103007.
- [12] V. Nguyen-Van, B. Panda, G. Zhang, H. Nguyen-Xuan, and P. Tran, "Digital design computing and modelling for 3-D concrete printing," *Automation in Construction*, vol. 123, 2021, doi: 10.1016/j.autcon.2020.103529.
- [13] A. Ahmed, A. Azam, M. M. Aslam Bhutta, F. A. Khan, R. Aslam, and Z. Tahir, "Discovering the technology evolution pathways for 3D printing (3DP) using bibliometric investigation and emerging applications of 3DP during COVID-19," *Cleaner Environmental Systems*, vol. 3, 2021, doi: 10.1016/j.cesys.2021.100042.



- [14] S. Luhar *et al.*, "Sustainable and Renewable Bio-Based Natural Fibres and Its Application for 3D Printed Concrete: A Review," *Sustainability*, vol. 12, no. 24, 2020, doi: 10.3390/su122410485.
- [15] D. Delgado Camacho *et al.*, "Applications of additive manufacturing in the construction industry – A forward-looking review," *Automation in Construction*, vol. 89, pp. 110-119, 2018, doi: 10.1016/j.autcon.2017.12.031.
- [16] T. Suntharalingam *et al.*, "Numerical Study of Fire and Energy Performance of Innovative Light-Weight 3D Printed Concrete Wall Configurations in Modular Building System," *Sustainability*, vol. 13, no. 4, 2021, doi: 10.3390/su13042314.
- [17] T. Suntharalingam *et al.*, "Energy Performance of 3D-Printed Concrete Walls: A Numerical Study," *Buildings*, vol. 11, no. 10, 2021, doi: 10.3390/buildings11100432..
- [18] S. Hayes, C. Desha, and D. Baumeister, "Learning from nature – Biomimicry innovation to support infrastructure sustainability and resilience," *Technological Forecasting and Social Change*, vol. 161, 2020, doi: 10.1016/j.techfore.2020.120287.
- [19] A. du Plessis *et al.*, "Beautiful and Functional: A Review of Biomimetic Design in Additive Manufacturing," *Additive Manufacturing*, vol. 27, pp. 408-427, 2019, doi: 10.1016/j.addma.2019.03.033.
- [20] M. K. Islam, P. J. Hazell, J. P. Escobedo, and H. Wang, "Biomimetic armour design strategies for additive manufacturing: A review," *Materials & Design*, vol. 205, 2021, doi: 10.1016/j.matdes.2021.109730.
- [21] Z. Jia and L. Wang, "3D printing of biomimetic composites with improved fracture toughness," *Acta Materialia*, vol. 173, pp. 61-73, 2019, doi: 10.1016/j.actamat.2019.04.052.
- [22] K. Ko, S. Jin, S. E. Lee, I. Lee, and J.-W. Hong, "Bio-inspired bimaterial composites patterned using three-dimensional printing," *Composites Part B: Engineering*, vol. 165, pp. 594-603, 2019, doi: 10.1016/j.compositesb.2019.02.008.
- [23] A. du Plessis, A. J. Babafemi, S. C. Paul, B. Panda, J. P. Tran, and C. Broeckhoven, "Biomimicry for 3D concrete printing: A review and perspective," *Additive Manufacturing*, vol. 38, 2021, doi: 10.1016/j.addma.2020.101823.
- [24] L. Wang, H. Jiang, Z. Li, and G. Ma, "Mechanical behaviors of 3D printed lightweight concrete structure with hollow section," *Archives of Civil and Mechanical Engineering*, vol. 20, no. 1, 2020, doi: 10.1007/s43452-020-00017-1.
- [25] B. Panda, M. Leite, B. B. Biswal, X. Niu, and A. Garg, "Experimental and numerical modelling of mechanical properties of 3D printed honeycomb structures," *Measurement*, vol. 116, pp. 495-506, 2018, doi: 10.1016/j.measurement.2017.11.037.
- [26] M. Moini, J. Olek, J. P. Youngblood, B. Magee, and P. D. Zavattieri, "Additive Manufacturing and Performance of Architected Cement-Based Materials," *Adv Mater*, vol. 30, no. 43, p. e1802123, Oct 2018, doi: 10.1002/adma.201802123.
- [27] M. H. Rashid, M. Molla, and I. M Taki, "Effect of Elevated Temperature on Bond Strength of Concrete." In *Materials Science Forum*, vol. 972, pp. 26-33. Trans Tech Publications Ltd, 2019.
- [28] I. R. Upasiri, K. M. C. Konthesigha, S. M. A. Nanayakkara, K. Poologanathan, P. Gatheeshgar, and D. Nuwanthika, "Finite element analysis of lightweight composite

- sandwich panels exposed to fire," *Journal of Building Engineering*, vol. 40, 2021, doi: 10.1016/j.jobbe.2021.102329.
- [29] A. Z. Mohd Ali, J. Sanjayan, and M. Guerrieri, "Performance of geopolymer high strength concrete wall panels and cylinders when exposed to a hydrocarbon fire," *Construction and Building Materials*, vol. 137, pp. 195-207, 2017, doi: 10.1016/j.conbuildmat.2017.01.099.
- [30] T. Suntharalingam *et al.*, "Fire performance of innovative 3D printed concrete composite wall panels – A Numerical Study," *Case Studies in Construction Materials*, vol. 15, 2021, doi: 10.1016/j.cscm.2021.e00586.
- [31] J. J. del Coz-Díaz, J. E. Martínez-Martínez, M. Alonso-Martínez, and F. P. Álvarez Rabanal, "Comparative study of LightWeight and Normal Concrete composite slabs behaviour under fire conditions," *Engineering Structures*, vol. 207, 2020, doi: 10.1016/j.engstruct.2020.110196.
- [32] S. Banerji, V. Kodur, and R. Solhmirzaei, "Experimental behavior of ultra high performance fiber reinforced concrete beams under fire conditions," *Engineering Structures*, vol. 208, 2020, doi: 10.1016/j.engstruct.2020.110316.
- [33] P. Weerasinghe, K. Nguyen, P. Mendis, and M. Guerrieri, "Large-scale experiment on the behaviour of concrete flat slabs subjected to standard fire," *Journal of Building Engineering*, vol. 30, 2020, doi: 10.1016/j.jobbe.2020.101255.
- [34] V. D. Cao, T. Q. Bui, and A.-L. Kjøniksen, "Thermal analysis of multi-layer walls containing geopolymer concrete and phase change materials for building applications," *Energy*, vol. 186, 2019, doi: 10.1016/j.energy.2019.07.122.
- [35] E. Steau, M. Mahendran, and K. Poologanathan, "Elevated temperature thermal properties of carbon steels used in cold-formed light gauge steel frame systems," *Journal of Building Engineering*, vol. 28, 2020, doi: 10.1016/j.jobbe.2019.101074.
- [36] S. Gunalan and M. Mahendran, "Fire performance of cold-formed steel wall panels and prediction of their fire resistance rating," *Fire Safety Journal*, vol. 64, pp. 61-80, 2014, doi: 10.1016/j.firesaf.2013.12.003.
- [37] E. Steau, M. Mahendran, and K. Poologanathan, "Experimental study of fire resistant board configurations under standard fire conditions," *Fire Safety Journal*, vol. 116, 2020, doi: 10.1016/j.firesaf.2020.103153.
- [38] S. Gunalan, P. Kolarkar, and M. Mahendran, "Experimental study of load bearing cold-formed steel wall systems under fire conditions," *Thin-Walled Structures*, vol. 65, pp. 72-92, 2013, doi: 10.1016/j.tws.2013.01.005.
- [39] A. D. Ariyanayagam and M. Mahendran, "Experimental study of load-bearing cold-formed steel walls exposed to realistic design fires," *Journal of Structural Fire Engineering*. 2014.
- [40] A. D. Ariyanayagam and M. Mahendran, "Fire design rules for load bearing cold-formed steel frame walls exposed to realistic design fire curves," *Fire Safety Journal*, vol. 77, pp. 1-20, 2015, doi: 10.1016/j.firesaf.2015.05.007.
- [41] A. D. Ariyanayagam and M. Mahendran, "Influence of cavity insulation on the fire resistance of light gauge steel framed walls," *Construction and Building Materials*, vol. 203, pp. 687-710, 2019, doi: 10.1016/j.conbuildmat.2019.01.076.

- [42] A. D. Ariyanayagam and M. Mahendran, "Experimental study of non-load bearing light gauge steel framed walls in fire," *Journal of Constructional Steel Research*, vol. 145, pp. 529-551, 2018, doi: 10.1016/j.jcsr.2018.02.023.
- [43] Y. Dias, P. Keerthan, and M. Mahendran, "Fire performance of steel and plasterboard sheathed non-load bearing LSF walls," *Fire Safety Journal*, vol. 103, pp. 1-18, 2019, doi: 10.1016/j.firesaf.2018.11.005.
- [44] S. Kesawan and M. Mahendran, "Fire tests of load-bearing LSF walls made of hollow flange channel sections," *Journal of Constructional Steel Research*, vol. 115, pp. 191-205, 2015, doi: 10.1016/j.jcsr.2015.07.020.
- [45] S. Kesawan and M. Mahendran, "Fire design rules for LSF walls made of hollow flange channel sections," *Thin-Walled Structures*, vol. 107, pp. 300-314, 2016, doi: 10.1016/j.tws.2016.05.022.
- [46] D. Perera *et al.*, "Fire performance of cold, warm and hybrid LSF wall panels using numerical studies," *Thin-Walled Structures*, vol. 157, 2020, doi: 10.1016/j.tws.2020.107109.
- [47] A. D. Ariyanayagam and M. Mahendran, "Numerical modelling of load bearing light gauge steel frame wall systems exposed to realistic design fires," *Thin-Walled Structures*, vol. 78, pp. 148-170, 2014, doi: 10.1016/j.tws.2014.01.003.
- [48] S. Gunalan and M. Mahendran, "Finite element modelling of load bearing cold-formed steel wall systems under fire conditions," *Engineering Structures*, vol. 56, pp. 1007-1027, 2013, doi: 10.1016/j.engstruct.2013.06.022.
- [49] P. Keerthan and M. Mahendran, "Thermal Performance of Composite Panels Under Fire Conditions Using Numerical Studies: Plasterboards, Rockwool, Glass Fibre and Cellulose Insulations," *Fire Technology*, vol. 49, no. 2, pp. 329-356, 2012, doi: 10.1007/s10694-012-0269-6.
- [50] T. Suntharalingam *et al.*, "Fire resistance of 3D printed concrete composite wall panels exposed to various fire scenarios," *Journal of Structural Fire Engineering*, vol. ahead-of-print, no. ahead-of-print, 2021, doi: 10.1108/jsfe-10-2020-0029.
- [51] J. Xiao, N. Han, L. Zhang, and S. Zou, "Mechanical and microstructural evolution of 3D printed concrete with polyethylene fiber and recycled sand at elevated temperatures," *Construction and Building Materials*, vol. 293, 2021, doi: 10.1016/j.conbuildmat.2021.123524.
- [52] Y. Weng *et al.*, "Printability and fire performance of a developed 3D printable fibre reinforced cementitious composites under elevated temperatures," *Virtual and Physical Prototyping*, vol. 14, no. 3, pp. 284-292, 2018, doi: 10.1080/17452759.2018.1555046.
- [53] A. Cicione, J. Kruger, R. S. Walls, and G. Van Zijl, "An experimental study of the behavior of 3D printed concrete at elevated temperatures," *Fire Safety Journal*, vol. 120, 2021, doi: 10.1016/j.firesaf.2020.103075.
- [54] A. Cicione, K. Mazolwana, J. Kruger, R. Walls, Z. Sander, and G. Van Zijl, "Effect of transverse and longitudinal confinement on the interlayer bond in 3D printed concrete at elevated temperatures: an experimental study," presented at the Proceedings of the 11th International Conference on Structures in Fire (SiF2020), 2020.
- [55] J. Sun, J. Xiao, Z. Li, and X. Feng, "Experimental study on the thermal performance of a 3D printed concrete prototype building," *Energy and Buildings*, vol. 241, 2021, doi: 10.1016/j.enbuild.2021.110965.

- [56] M. Kaszynka *et al.*, "Thermal-humidity parameters of 3D printed wall," *InIOP Conference Series: Materials Science and Engineering*, Vol. 471, No. 8, p. 082018, IOP Publishing, 2019
- [57] S. Yang, S. Wi, J. H. Park, H. M. Cho, and S. Kim, "Novel proposal to overcome insulation limitations due to nonlinear structures using 3D printing: Hybrid heat-storage system," *Energy and Buildings*, vol. 197, pp. 177-187, 2019, doi: 10.1016/j.enbuild.2019.05.048.
- [58] A. S. Alchaar and A. K. Al-Tamimi, "Mechanical properties of 3D printed concrete in hot temperatures," *Construction and Building Materials*, vol. 266, 2021, doi: 10.1016/j.conbuildmat.2020.120991.
- [59] H. Marais, H. Christen, S. Cho, W. De Villiers, and G. Van Zijl, "Computational assessment of thermal performance of 3D printed concrete wall structures with cavities," *Journal of Building Engineering*, vol. 41, 2021, doi: 10.1016/j.job.2021.102431.
- [60] M. Mahadevan, A. Francis, and A. Thomas, "A simulation-based investigation of sustainability aspects of 3D printed structures," *Journal of Building Engineering*, vol. 32, 2020, doi: 10.1016/j.job.2020.101735.
- [61] Hibbett, Karlsson, and Sorensen, *ABAQUS/standard: User's Manual*. Vol. 1, 1998
- [62] European Committee for Standardisation, "EN 1993-1-2: Eurocode 3: Design of steel structures - Part 1-2: General rules - Structural fire design".
- [63] I. Upasiri, C. Konthesingha, A. Nanayakkara, K. Poologanathan, B. Nagaratnam, and G. Perampalam, "Evaluation of fire performance of lightweight concrete wall panels using finite element analysis," *Journal of Structural Fire Engineering*, vol. ahead-of-print, no. ahead-of-print, 2021, doi: 10.1108/jsfe-10-2020-0030.
- [64] I. Upasiri, C. Konthesingha, K. Poologanathan, A. Nanayakkara, and B. Nagaratnam, "Review on Fire Performance of Cellular Lightweight Concrete," *ICSBE 2018*, R. Dissanayake, and P. Mendis, eds., Springer Singapore, Singapore, 2020, pp. 470–478.
- [65] X. Tan *et al.*, "Influence of high temperature on the residual physical and mechanical properties of foamed concrete," *Construction and Building Materials*, vol. 135, pp. 203-211, 2017, doi: 10.1016/j.conbuildmat.2016.12.223.
- [66] K. Ramamurthy, E. K. Kunhanandan Nambiar, and G. Indu Siva Ranjani, "A classification of studies on properties of foam concrete," *Cement and Concrete Composites*, vol. 31, no. 6, pp. 388-396, 2009, doi: 10.1016/j.cemconcomp.2009.04.006.
- [67] European Committee for Standardisation, "EN 1991-1-2: Eurocode 1: Actions on structures - Part 1-2: General actions - Actions on structures exposed to fire".
- [68] American Society for Testing and Materials, "ASTM E119: Standard Test Methods for Fire Tests of Building Construction and Materials"
- [69] A. D. Ariyanayagam and M. Mahendran, "Development of realistic design fire time-temperature curves for the testing of cold-formed steel wall systems," *Frontiers of Structural and Civil Engineering*, vol. 8, no. 4, pp. 427-447, 2014, doi: 10.1007/s11709-014-0279-1.